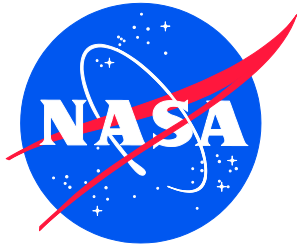


NASA/TM-2019-220412  
NESC-RP-19-01416



# Large Male Anthropomorphic Test Device (ATD) Finite Element Model (FEM) Correlation Improvement

*Michael J. Kelly/NESC  
Langley Research Center, Hampton, Virginia*

*Jeffrey T. Somers  
KBR, Houston, Texas*

*Jacob B. Putnam  
Langley Research Center, Hampton, Virginia*

*Preston C. Greenhalgh  
KBR, Houston, Texas*

*Charles Lawrence  
Analytical Mechanics Associates, Hampton, Virginia*

## NASA STI Program . . . in Profile

Since its founding, NASA has been dedicated to the advancement of aeronautics and space science. The NASA scientific and technical information (STI) program plays a key part in helping NASA maintain this important role.

The NASA STI program operates under the auspices of the Agency Chief Information Officer. It collects, organizes, provides for archiving, and disseminates NASA's STI. The NASA STI program provides access to the NTRS Registered and its public interface, the NASA Technical Reports Server, thus providing one of the largest collections of aeronautical and space science STI in the world. Results are published in both non-NASA channels and by NASA in the NASA STI Report Series, which includes the following report types:

- **TECHNICAL PUBLICATION.** Reports of completed research or a major significant phase of research that present the results of NASA Programs and include extensive data or theoretical analysis. Includes compilations of significant scientific and technical data and information deemed to be of continuing reference value. NASA counter-part of peer-reviewed formal professional papers but has less stringent limitations on manuscript length and extent of graphic presentations.
- **TECHNICAL MEMORANDUM.** Scientific and technical findings that are preliminary or of specialized interest, e.g., quick release reports, working papers, and bibliographies that contain minimal annotation. Does not contain extensive analysis.
- **CONTRACTOR REPORT.** Scientific and technical findings by NASA-sponsored contractors and grantees.

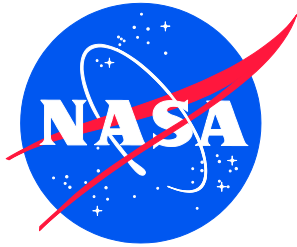
- **CONFERENCE PUBLICATION.** Collected papers from scientific and technical conferences, symposia, seminars, or other meetings sponsored or co-sponsored by NASA.
- **SPECIAL PUBLICATION.** Scientific, technical, or historical information from NASA programs, projects, and missions, often concerned with subjects having substantial public interest.
- **TECHNICAL TRANSLATION.** English-language translations of foreign scientific and technical material pertinent to NASA's mission.

Specialized services also include organizing and publishing research results, distributing specialized research announcements and feeds, providing information desk and personal search support, and enabling data exchange services.

For more information about the NASA STI program, see the following:

- Access the NASA STI program home page at <http://www.sti.nasa.gov>
- E-mail your question to [help@sti.nasa.gov](mailto:help@sti.nasa.gov)
- Phone the NASA STI Information Desk at 757-864-9658
- Write to:  
NASA STI Information Desk  
Mail Stop 148  
NASA Langley Research Center  
Hampton, VA 23681-2199

NASA/TM-2019-220412  
NESC-RP-19-01416



# Large Male Anthropomorphic Test Device (ATD) Finite Element Model (FEM) Correlation Improvement

*Michael J. Kelly/NESC  
Langley Research Center, Hampton, Virginia*

*Jeffrey T. Somers  
KBR, Houston, Texas*

*Jacob B. Putnam  
Langley Research Center, Hampton, Virginia*

*Preston C. Greenhalgh  
KBR, Houston, Texas*

*Charles Lawrence  
Analytical Mechanics Associates, Hampton, Virginia*

National Aeronautics and  
Space Administration

Langley Research Center  
Hampton, Virginia 23681-2199

October 2019

## **Acknowledgments**

The NESC assessment team would like to acknowledge the team at Livermore Software Technology Corporation (LSTC) who provided support on the large male ATD FEM throughout this project: Mr. Christoph Maurath and Mr. Eric Day. The assessment team would also like to acknowledge peer reviewers Mr. Martin Annett and Mr. Jonathan Austin, who contributed their time and energy to improve this report.

The use of trademarks or names of manufacturers in the report is for accurate reporting and does not constitute an official endorsement, either expressed or implied, of such products or manufacturers by the National Aeronautics and Space Administration.

Available from:

NASA STI Program / Mail Stop 148  
NASA Langley Research Center  
Hampton, VA 23681-2199  
Fax: 757-864-6500



## **NASA Engineering and Safety Center Technical Assessment Report**

# **Large Male Anthropomorphic Test Device (ATD) Finite Element Model (FEM) Correlation Improvement**

**August 29, 2019**

## Report Approval and Revision History

NOTE: This document was approved at the August 29, 2019, NRB. This document was submitted to the NESC Director on September 3, 2019, for configuration control.

Approved:	<i>Original Signature on File (MK)</i>	9/4/19
	NESC Director	Date

Version	Description of Revision	Office of Primary Responsibility	Effective Date
1.0	Initial Release	Michael J. Kelly, NESC Associate Principal Engineer, LaRC	8/29/19

## Table of Contents

1.0	Notification and Authorization .....	6
2.0	Signature Page .....	7
3.0	Team List .....	8
3.1	Acknowledgments .....	8
4.0	Executive Summary .....	9
5.0	Assessment Plan.....	10
6.0	Problem Description and Proposed Solutions.....	10
7.0	Data Analysis .....	12
7.1	Development of Geometrically Accurate Head-Neck Complex.....	12
7.2	Optimization of Neck Material Parameters .....	13
7.3	Verification of Large Male ATD FEM Correlation Improvement .....	20
8.0	Findings and Observations.....	25
8.1	Findings .....	25
8.2	Observations .....	25
9.0	Alternative Viewpoint(s) .....	25
10.0	Other Deliverables .....	25
11.0	Lessons Learned.....	26
12.0	Recommendations for NASA Standards and Specifications .....	26
13.0	Definition of Terms.....	26
14.0	Acronyms and Nomenclature .....	26
15.0	References.....	27
	Appendices.....	27

## List of Figures

Figure 6.0-1. Baseline Correlation Comparison—Lateral Impact 6 g 100ms .....	11
Figure 6.0-2. Comparison of Hybrid III Medium and Large Male ATD Neck Configurations ...	11
Figure 7.1-1. Developmental Process for Building Geometrically Accurate Large Male Neck FEM .....	12
Figure 7.1-2. Depiction of Measurements Taken to Verify Head-Form FEM Geometry .....	13
Figure 7.2-1. FEM Prediction of Neck Upper Z-Force with Constant Stress (left) and Fully Integrated (right) Elements in Neck Puck Part .....	14
Figure 7.2-2. Sensitivity Assessment between Baseline and Upper Parameter Bound FEM under Frontal Loading: 10 g–50 ms.....	16
Figure 7.2-3. Flowchart of Optimization Procedure—Lateral Optimization .....	17
Figure 7.2-4. Correlation Comparison between Baseline and Lateral Optimized FEM under Lateral Loading: 6 g–100 ms (top) and 12 g–100 ms (right).....	18
Figure 7.2-5. Correlation Comparison between Lateral and Rearward Optimized FEM under Rearward Loading: 6 g–100 ms (left) and 16 g–50 ms (right) .....	19
Figure 7.2-6. Correlation Comparison between Rearward and Manual Optimized FEM under Lateral: 6 g–100 ms (top left) and 12 g–50 ms (top right) and Rearward Loading: 6 g–100 ms (bottom left) and 16 g–50 ms (bottom right).....	20
Figure 7.3-1. Verification of Material Calibration under Frontal Loading: 6 g–100 ms (top), 16 g–50 ms (middle), 8 g–50 ms at 20° (bottom).....	21
Figure 7.3-2. Verification of Material Calibration with Full Boundary Conditions Implementation under Lateral: 6 g–100 ms (top left) and 12 g–50 ms (top right) and Rearward Loading: 6 g–100 ms (bottom left) and 16 g–50 ms (bottom right).....	22
Figure 7.3-3. Updated Head-Neck Complex Integrated into Hybrid III Large Male FEM.....	24
Figure A-1. Test 9704: Frontal Impact 6-g 50ms .....	28
Figure A2. Test 9740: Frontal Impact 8-g 50ms.....	29
Figure A3. Test 9708: Frontal Impact 10-g 100ms.....	30
Figure A4: Test 9713: Frontal Impact 12-g 100ms .....	31
Figure A5: Test 9741: Frontal Impact 12-g 50ms .....	32
Figure A6. Test 9742: Frontal Impact 16-g 50ms.....	33
Figure A7. Test 9702: Rearward Impact 6-g 100ms.....	34
Figure A8. Test 9712: Rearward Impact 8-g 100ms.....	35
Figure A9. Test 9734: Rearward Impact 8-g 50ms.....	36
Figure A10. Test 9706: Rearward Impact 10-g 100ms.....	37
Figure A11. Test 9735: Rearward Impact 12-g 50ms.....	38
Figure A12. Test 9711: Rearward Impact 12-g 100ms.....	39
Figure A13. Test 9736: Rearward Impact 16-g 50ms.....	40
Figure A14. Test 9703: Lateral Impact 6-g 100ms.....	41
Figure A15. Test 9737: Lateral Impact 8-g 50ms.....	42
Figure A16. Test 9739: Lateral Impact 10-g 100ms.....	43

Figure A17. Test 9739: Lateral Impact 10-g 50ms.....	44
Figure A18. Test 9714: Lateral Impact 12-g 100ms.....	45
Figure A19. Test 9738: Lateral 12-g 50ms.....	46
Figure A20. Test 9743: Combined Frontal-Lateral Impact 8-g 50ms .....	48
Figure A21. Test 9744: Combined Frontal Lateral Impact 12-g 50ms.....	49
Figure A22. Test 9745: Combined Frontal-Lateral Impact 16-g 50ms .....	51
Figure A23. Test 9746: Combined Rearward-Lateral Impact 8-g 50ms .....	52
Figure A24. Test 9747: Combined Rearward-Lateral Impact 12-g 50ms .....	54
Figure A25. Test 9748: Combined Rearward-Lateral Impact 16-g 50ms .....	55

### **List of Tables**

Table 7.1-1. Geometry and Mass Measurements of Head-Form.....	13
Table 7.2-1. Large Male ATD Isolated Head-Neck Test Matrix.....	14
Table 7.2-2. Material Parameters Used in the Sensitivity Analysis .....	15
Table 7.2-3. Optimized Parameters—Lateral Optimization.....	18
Table 7.2-4. Optimized Parameters—Rearward Optimization.....	19
Table 7.2-5. Optimized Parameters—Manual Optimization .....	20
Table 7.3-1. ISO/TR 16250:2013 Rating for Each Response Predicted by Baseline FEM.....	23
Table 7.3-2. ISO/TR 16250:2013 Rating for Each Response Predicted by Updated FEM.....	23

# Technical Assessment Report

## 1.0 Notification and Authorization

In October 2018, as part of an activity for the Commercial Crew Program (CCP), a NASA Engineering and Safety Center (NESC) team conducted tests of small female, medium male, and large male Hybrid III anthropomorphic test device (ATD) head-neck complexes at Wright-Patterson Air Force Base<sup>1</sup>. The results were compared to simulation results from ATD finite element model (FEM) predictions to determine the validity and fidelity of ATD models for use in certifying CCP vehicles. Mr. Jeff Suhey, Multi-Purpose Crew Vehicle (MPCV) LS-DYNA analyst, requested the NESC help improve the large male ATD FEM to better represent physical responses. This would be accomplished via changes to material model parameters, geometry, and/or mass properties of the head and neck to improve the correlation with physical test data collected during previous NESC testing. The improved model will provide the MPCV Program with reliable FEMs when performing occupant protection analysis for large occupants.

The key stakeholders for this assessment are the Human Exploration and Operations Mission Directorate, the CCP, and Lockheed Martin.

---

<sup>1</sup> NESC TI-16-01162, Evaluation of Occupant Protection Requirement Verification Approach by CCP Partners



### 3.0 Team List

Name	Discipline	Organization
<b>Core Team</b>		
Mike Kelly	NESC Lead	LaRC
Jeff Somers	Technical Lead	JSC/KBR
Jacob Putnam	Analyst	LaRC
Preston Greenhalgh	Analyst	JSC/KBR
<b>Consultants</b>		
Charles Lawrence	Consultant	LaRC/AMA
<b>Business Management</b>		
Becki Hendricks	Program Analyst	LaRC/MTSO
<b>Assessment Support</b>		
Linda Burgess	Planning and Control Analyst	LaRC/AMA
Jenny DeVasher	Technical Editor	LaRC/AS&M
Betty Trebaol	Project Coordinator	LaRC/AMA

### 3.1 Acknowledgments

The NESC assessment team would like to acknowledge the team at Livermore Software Technology Corporation (LSTC) who provided support on the large male ATD FEM throughout this project: Mr. Christoph Maurath and Mr. Eric Day. The assessment team would also like to acknowledge peer reviewers Mr. Martin Annett and Mr. Jonathan Austin, who contributed their time and energy to improve this report.

## 4.0 Executive Summary

The NESC updated the LSTC finite element model (FEM) of the Hybrid III large male ATD head-neck complex for use in occupant protection analysis of the Multi-Purpose Crew Vehicle (MPCV) Orion Crew Module (CM). This model is an essential component of the predictive tools used to determine the risk of crew injury under dynamic loading, with its outputs being used to quantify head and neck injury risk. The validity of these predictions is predicated on the FEM being an accurate representation of the physical ATD it represents.

The previous FEM of the large male ATD head-neck complex was found to poorly represent the physical ATD when correlating to a series of isolated head-neck sled tests performed by the NESC (i.e., NESC TI-16-01162). The physical ATD exhibited a stiffer response under front, rearward, and lateral loading than the FEM. Evaluation of the FEM indicated lack of correlation stemmed from differences in neck geometry and material properties between the FEM and physical ATD.

To improve the correlation of the large male ATD FEM, the geometry of the neck model was updated to match the physical device. The geometry of each part was resized, and spacer parts were added to match the neck parts used in the device. Mass was added to the FEM head-form to match the ATD design specifications. Geometry of the updated head-neck FEM was verified against measurements taken on the device.

After updating the FEM geometry and mass, a material calibration was performed to improve the FEM prediction of the physical ATD test data. Three optimizations were performed to calibrate the parameters used to define the shear modulus of the neck puck material in the FEM. Post calibration, the updated head-neck FEM was assessed against head-neck test data through qualitative evaluation and the quantitative curve correlation metrics.

The updated large male head-neck FEM closely predicted the physical ATD in all test conditions evaluated. Significant improvement was shown, with 97.5% of responses from the updated FEM exhibiting adequate correlation, compared to 45% in the original FEM, quantified using the ISO/TR 16250 *Road Vehicles—Objective Rating Metrics for Dynamic Systems* curve rating system.

In summary, the Hybrid III large male ATD head-neck FEM was updated to better match the geometric and material properties of the physical device. The graphs contained in Appendix A demonstrate improved predictive accuracy under lateral, rear, and frontal impact conditions with combined horizontal and vertical loading. The improved accuracy of this FEM increases confidence in its use for occupant protection evaluation of large male occupants.

## 5.0 Assessment Plan

This NESC assessment included the following proposed tasks:

1. Investigate differences between the physical ATD and FEM in head-neck geometry, mass, and material properties. [Section 7.1]
2. Update geometry and mass properties to match physical large male ATD. [Section 7.1]
  - For difference in neck, use medium male FEM neck as starting point.
  - Add FEM spacers to match physical ATD configuration.
3. Conduct optimization study to determine material properties. [Section 7.2]
4. Assess correlation of updated FEM against existing head-neck test data, using existing head-neck sled test data for correlation comparison. [Section 7.3]

The intended scope of deliverables included correlated large male ATD FEM and documentation, to be delivered to the requester. The MPCV Program will use the updated FEM to assess crew injury risk in the combined suit and seat modeling assessment needed for the suit critical design review, scheduled for September 2019. Results will also be provided to the ATD FEM commercial developer (i.e., LSTC) for incorporation into future releases.

## 6.0 Problem Description and Proposed Solutions

The LSTC Hybrid III large male ATD FEM [ref. 1] was found to correlate poorly to a series of isolated head-neck tests by the NESC (i.e., NESC TI-16-01162). In these tests, the head-neck was fixed to a sled and accelerated; all responses were driven by inertial loading. This setup limited environmental variability and allowed a direct measure of ATD response with which to evaluate the FEM. The FEM exhibited increased compliance compared to the physical ATD, resulting in overprediction of ATD response and limited viability in predicting occupant injury risk. This poor correlation is demonstrated by the incorrect peak and shape of response for head rotational velocity under lateral loading shown in Figure 6.0-1. Figure 6.0-2 These results were presented to the analysts who are using this model to conduct occupant protection simulations for certification of the MPCV CM.

Based on this data, the NESC was requested to assess and improve the FEM correlation. The NESC assessment team's initial objective was to identify discrepancies between the physical ATD and the FEM. Initial evaluation identified two primary discrepancies. First, the FEM neck component did not match the ATD physical geometry. Second, the material model parameters for FEM neck parts did not match the material used in the device. The focus of this assessment was to remedy these discrepancies and develop a more representative FEM of the Hybrid III large male ATD head-neck complex.

The proposed solution for developing a geometrically accurate head-neck complex was to build an updated neck complex model through an adaptation of the Hybrid III medium male ATD FEM [ref. 2]. The large male ATD neck is geometrically the same as the medium male ATD, with the exception of two spacer plate parts included in the large male ATD, which represent the longer neck length of the large male anthropometry. (Figure 6.0-2). Adding these spacer parts to the medium male neck FEM would result in an updated neck complex matching the physical dimensions of the large male ATD. The updated neck complex would be re-integrated with the

original large male head-complex model, and the dimensions and weights of the parts would be verified to ensure accuracy.

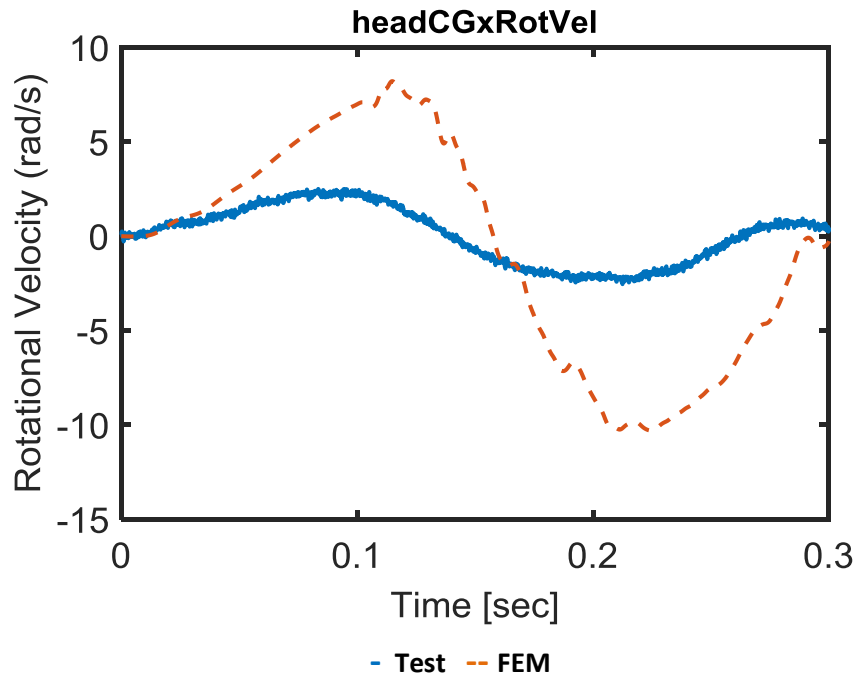


**Figure 6.0-1. Baseline Correlation Comparison—Lateral Impact 6 g 100ms**

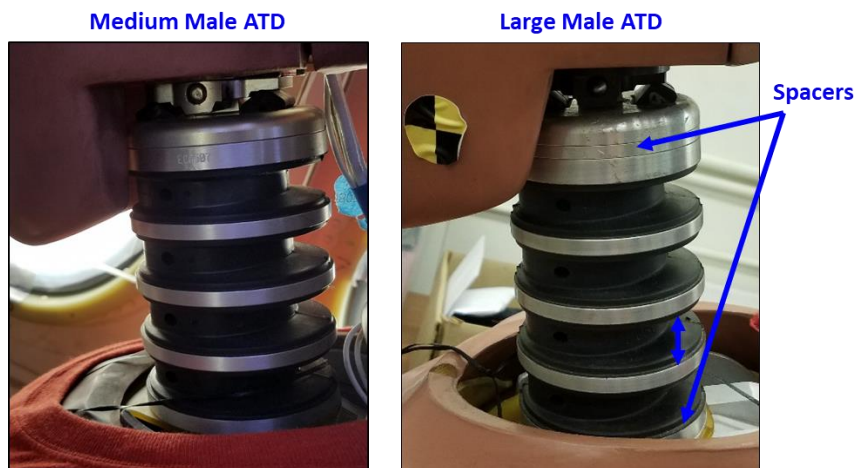


**Figure 6.0-2. Comparison of Hybrid III Medium and Large Male ATD Neck Configurations**

The proposed solution to calibrating the material discrepancies between physical ATD and FEM counterparts was to perform a material parameter optimization. The assessment team lacked access to the proprietary material specifications of the ATD neck parts, but it was known that the non-metallic material used in the neck pucks and occipital condyle (OC) joint nodding block is stiffer in the large male ATD than the material used in the medium male ATD. This stiffer material is used to approximate the increased musculature of the large male occupant. The material model parameters originally used to define these parts in the large male FEM were identical to those used in the medium male FEM. Because little information is publicly available for these materials, an optimization procedure was chosen to tune the original material model

parameters to match the response of the head-neck complex observed in the physical testing. The first step of the optimization was determining which of the material model parameters affected the ATD response. Next, the critical parameters would be optimized with a subset of test results to improve predictive response of the head-neck complex. The final calibrated FEM, with updated material model parameters, would be verified against all tests performed in the isolated head-neck test series.

## 7.0 Data Analysis

### 7.1 Development of Geometrically Accurate Head-Neck Complex

The neck complex was isolated from the LSTC Hybrid III medium male FEM version 151214\_beta [ref. 2] (see Figure 7.1-1). The height and radius of the neck parts in this model were compared to measurements taken on a Hybrid III large male ATD to verify the geometry of these parts matched between the two configurations. The two spacer plates in the large male ATD were modeled by extruding the upper and lower neck brackets one element depth of 0.2 in. The neck cable was lengthened to accommodate the resulting increase in distance between the upper neck and lower neck mounting brackets by which it is attached. After completion, the neck complex was integrated between the OC joint and lower neck assembly in the large male FEM. The final length of the updated neck FEM was verified again with measurements taken on the ATD.

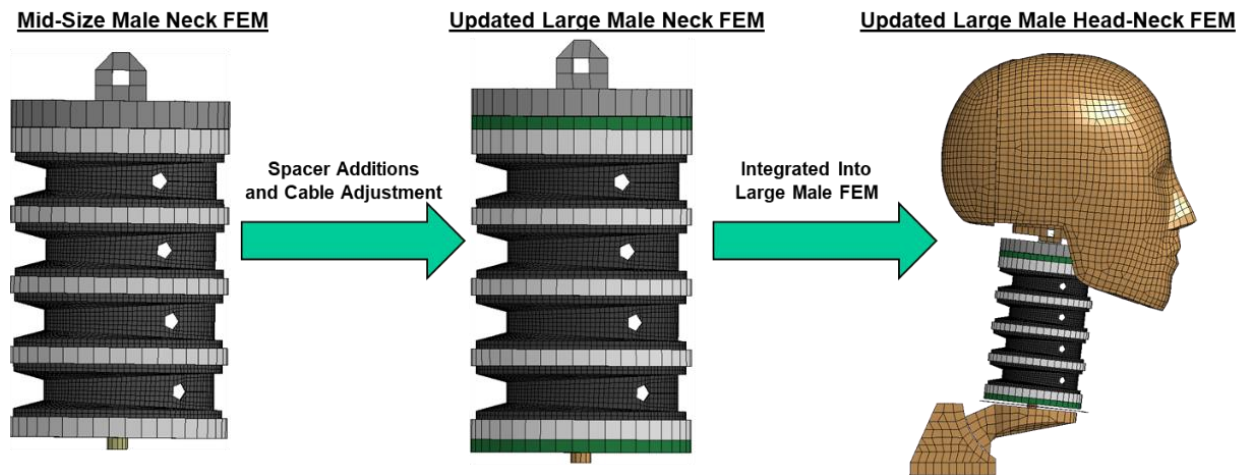


**Figure 7.1-1. Developmental Process for Building Geometrically Accurate Large Male Neck FEM**

The mass and geometry of the large male head complex FEM were compared to measurements publicly released by ATD manufacturer Humanetics [ref. 3]. The width and depth of the head form, taken as maximum distance across the sagittal and coronal plane (see Figure 7.1-2), were found to be within 0.1 in. of these measurements (Table 7.1-1). This difference was considered within resolution tolerance of the FEM mesh size and was not adjusted. A point mass of 0.53 lbs. was added to the FEM head center of gravity to bring its total weight within manufacturer specification tolerance.

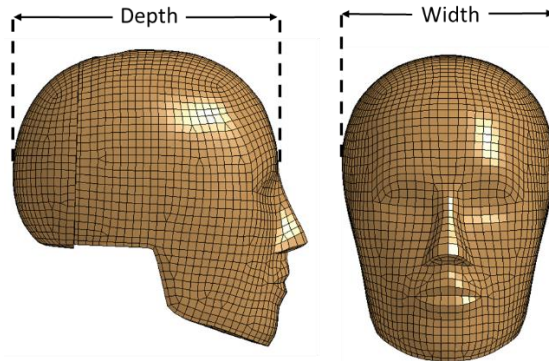


**Figure 7.1-2. Depiction of Measurements Taken to Verify Head-Form FEM Geometry**

**Table 7.1-1. Geometry and Mass Measurements of Head-Form**

Head Property	Physical ATD	Baseline FEM	Updated FEM
Head Depth (in)	7.87	7.95	No Change
Head Width (in)	6.10	6.14	No Change
Head Weight (lb.)	10.89 ± 0.11	10.27	10.80

## 7.2 Optimization of Neck Material Parameters

### 7.2.1 Optimization Procedure

Prior to calibrating the LSTC Hybrid III large male FEM, a series of baseline simulations were performed to evaluate the accuracy of the original FEM, the stability of the model, and sensitivity of the model’s response to perturbations during the simulation. To baseline the original FEM response, all isolated head-neck tests performed under NESC TI-16-01162 were simulated (Table 7.2-1). These tests were uniaxial sled tests in which the head-neck complex was oriented 40° from normal and accelerated in either the frontal, rearward, lateral, or combined front-lateral and rear-lateral directions. These loading conditions were chosen to elicit X (forward), Y (lateral), and Z (vertical) responses of the ATD. For each tested condition, ATD outputs were recorded and simulations were examined to verify model stability.

**Table 7.2-1. Large Male ATD Isolated Head-Neck Test Matrix**

	G level	Rise Time (ms)									
	Frontal	6		100	Rearward		6	100		Lateral	6
8		50	8	100		8	50	12	50		
10		100	8	50		10	100	16	50		
12		100	10	100		10	50	8	50		
12		50	12	50		12	100	12	50		
16		50	12	100		12	50	16	50		
			16	50							

Under later loading, the ATD FEM exhibited high-frequency noise in the upper neck force and head acceleration along the Z-direction at peak neck excursion. Hourglass issues in the neck puck elements were identified at the time of the spiking response. To correct this issue, the element definition of this part was changed from the default constant stress solid formulation to a fully integrated selectively reduced (S/R) solid. This improved the stability of these elements under high deformation and removed the high-frequency noise response predicted by the model (Figure 7.2-1).

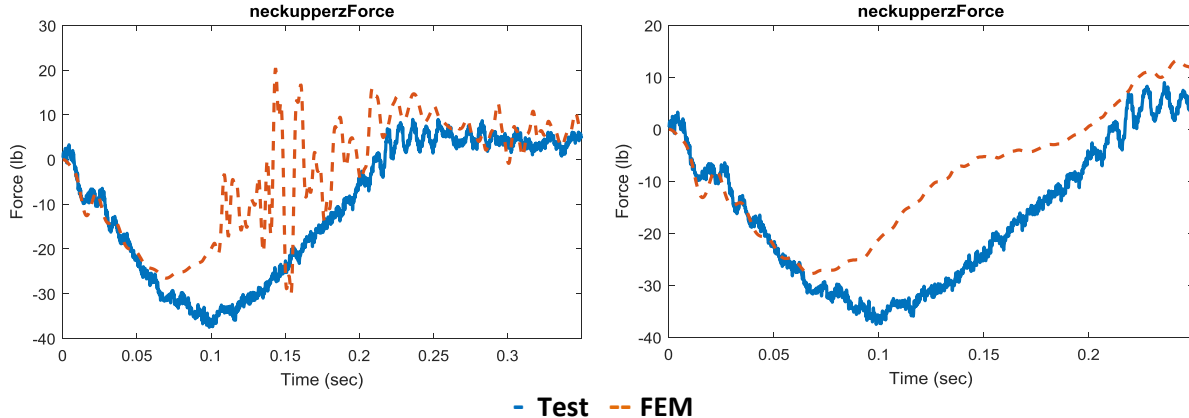


**Figure 7.2-1. FEM Prediction of Neck Upper Z-Force with Constant Stress (left) and Fully Integrated (right) Elements in Neck Puck Part**

A subset of cases in each impact direction were simulated with and without a 250 ms preload phase implemented prior to impact. This preload phase is simulated to allow the FEM time to reach a natural position under gravity and allow the tensioned cable within the neck to reach a steady load state. In the non-preload cases, the neck cable tension was removed to prevent response oscillations stemming from initialization of the neck cable. This cable tension is designed to prevent the head from separating from the neck under extreme loading environments, and did not affect ATD response when removed from these simulations. The effect of the preload phase was found to be consistent and minimal across the cases evaluated. It was determined that the preload phase could be removed for the optimization simulations to reduce computational run

time. This preload phase is important in full ATD simulations to include the device seat position under gravity and harness load.

To determine the material model parameters best situated to improve response through optimization, a sensitivity analysis was conducted on components known to differ between the large and medium male ATD. These included the neck puck and OC joint nodding block material (Table 3). The neck puck material is defined as \*MAT\_VISCOELASTIC in the FEM; this formulation uses density, elastic bulk modulus, short- and long-term shear moduli, and a decay constant ( $\beta$ ) as material parameters. The density and modulus parameters were evaluated between the original value (lower bound) and the baseline value scaled by a factor of 10 (upper bound). The sensitivity was evaluated only in the increase of these parameters because the material was known to be stiffer than that originally modeled. It was assumed that the stiffer rubber would also be denser. Because the decay constant does not have as direct a relationship between magnitude and material stiffness, its value was ranged between one-half (lower bound) and double (upper bound) the original value to evaluate sensitivity. The OC joint nodding block is represented as a rotational joint with a defined rotation angle versus applied moment curve. This curve is nonlinear, with applied moment increasing exponentially as the rotation increases. Rather than redefining a new curve, the dependent value, applied moment per angle, was scaled using a single parameter to represent changes in the nodding block stiffness. Only an increase in stiffness from the original value was considered. The bounds for each parameter were chosen at what was considered the edge reasonable for each material based on experience with the FEM and the desired change in response. These bounds do not reflect a prediction of the final parameter value.

**Table 7.2-2. Material Parameters Used in the Sensitivity Analysis**

<b>Material Parameter</b>	<b>Material Definition</b>	<b>Upper Bound</b>	<b>Lower Bound</b>
Neck Rubber Bulk Modulus, $K$ [psi]	*MAT_VISCOELASTIC	1.61E5	1.61E4
Neck Rubber Density, $\rho$ [lb/in <sup>3</sup> ]	*MAT_VISCOELASTIC	0.40	0.04
Neck Rubber Short-term Shear Modulus, $G_0$ , [psi]	*MAT_VISCOELASTIC	6.67E3	6.67E2
Neck Rubber Long-term Shear Modulus, $G_l$ , [psi]	*MAT_VISCOELASTIC	1.45E3	1.16E2
Neck Rubber Decay Constant, $\beta$ , [ms <sup>-1</sup> ]	*MAT_VISCOELASTIC	0.2	0.05
Nodding Block Rotational Stiffness Scale Factor	*CONSTRAINED_JOINT	2.0	1.0

Each material parameter was varied independently between a lower and upper bound to detect sensitivity in the model due to change of that parameter. The sensitivity was determined qualitatively by evaluating response comparisons between test and simulation (Figure 7.2-2). In these simulations, varying the neck material bulk modulus and the nodding block stiffness had negligible effects on the head-neck response. Changing the neck material density reduced correlation and induced instability in the neck response. Exhibiting limited value in improving the model, these parameters were not chosen for calibration. However, the three parameters that made up the shear modulus of the neck material (i.e., short- and long-term shear moduli and  $\beta$ ) positively influenced the model head-neck response. All three exhibited potential to reduce the peak rotational response of the head to be more in line with the test data, thus these parameters were selected for optimization.

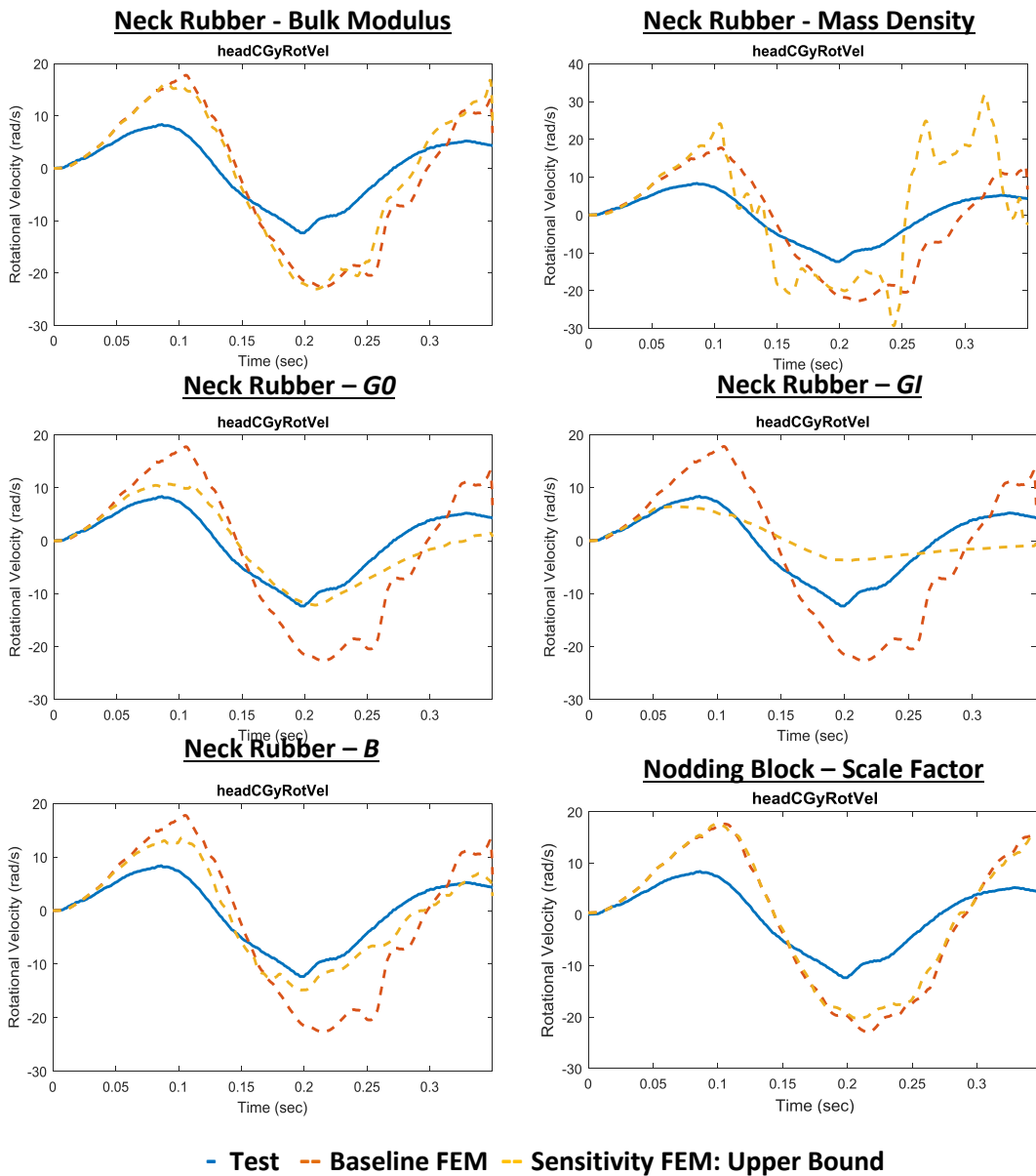


**Figure 7.2-2. Sensitivity Assessment between Baseline and Upper Parameter Bound FEM under Frontal Loading: 10 g–50 ms**

To calibrate the parameters used to define the shear modulus of the neck puck material, a step-wise property optimization was implemented. This consisted first of an optimization of FEM response under lateral loading, followed by an optimization of response under rearward loading. Each was conducted using a radial basis function network metamodel with a space-filling point selection implemented within LS-OPT [ref. 4]. This optimization methodology develops design surfaces to learn the effect of each variable on the objective response parameters. With each iteration, these surfaces were refined until an optimal variable set was selected. A flowchart of the optimization procedure is shown in Figure 7.2-3. Two test conditions, at the bounds of peak acceleration and rise times tested in each impact direction, were optimized simultaneously. This was done to prevent calibration biasing towards low- or high-energy impacts. For lateral loading

optimization, test cases with 6 g and 12 g peak acceleration with 100 ms and 50 ms rise times were used. For rearward loading, test cases with 6 g and 16 g peak acceleration with 100 ms and 50 ms rise times were used. For all cases, the head-neck complex was arranged at a 40° angle to the direction of load, matching the test setup orientation. Independent variables for the lateral optimization were the short- and long-term shear parameters ( $G0$  and  $GI$ ) of the neck pucker material model.

The results of this optimization were fed into the rearward optimization as new starting points for these variables, with  $\beta$  included as an independent variable in the rearward optimization. The objectives for the lateral optimization were selected to improve prediction of head rotational velocity and upper neck Z force. A total of 12 objectives were defined, including distinct peaks and time of peaks, for the head rotational velocity and neck Z force transient response. Results from the lateral optimization indicated convergence in the accuracy of the upper neck Z force in both directions. This objective was removed in the rearward optimization and replaced with additional objectives to improve the shape of the rotational velocity response. Four iterations were performed per optimization, resulting in a total of 40 and 72 simulations performed in the lateral and rearward optimizations, respectively. The difference in number of simulations performed is due to the additional independent variable in the rearward optimization increasing the number of variable designs per iteration from five to nine. Simulations were performed using LS-DYNA SMP Version R10.1.0 single precision. Simulations were run using four to eight processors on a Linux computer cluster. Simulations were executed to 0.3 second (s), with an average run time of approximately 7.5 hours.

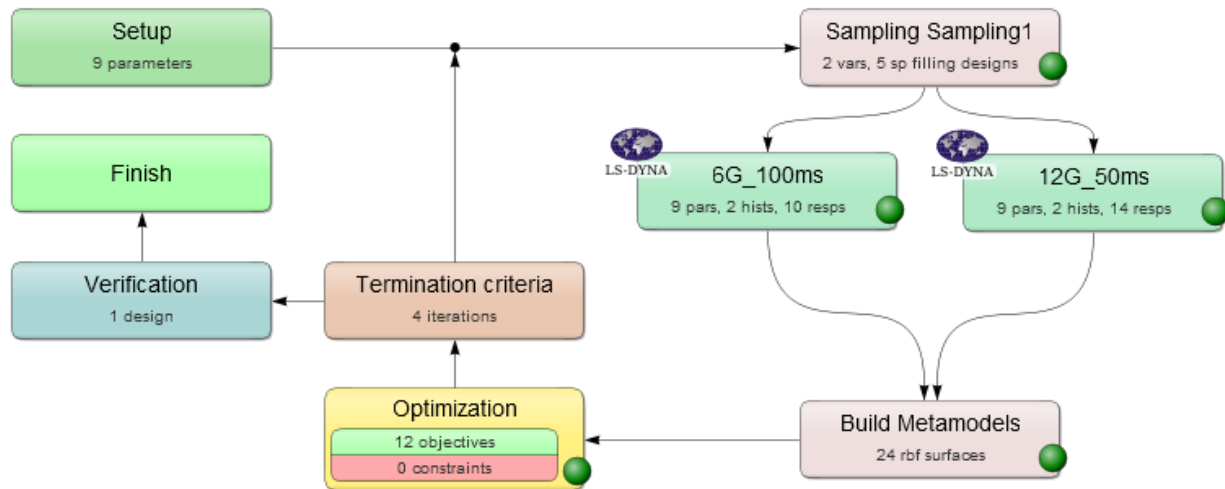


**Figure 7.2-3. Flowchart of Optimization Procedure—Lateral Optimization**

After completion of lateral and rear optimizations, a final manual calibration of the  $G0$ ,  $GI$ , and  $\beta$  parameters was performed. Based on previous optimizations, the effect of each parameter on the shape and size of the head rotational response was identified. Using this knowledge, each parameter was manually tuned to further improve the prediction of the ATD FEM response for the lateral and rear impact test conditions. The parameters were tuned with all four test conditions (i.e., two lateral and two rearward test conditions) being simulated in each iteration to ensure global improvement. Nine iterations were completed to reach a satisfactory response in all conditions evaluated. The effectiveness of each optimization was evaluated by a qualitative assessment of correlation rather than using more quantitative curve rating methodologies. The

more quantitative metrics do not prioritize correlation with the same objectives intended in each optimization, and thus were reserved for the verification phase.

### 7.2.2 Optimization Results

The initial optimization of the  $G0$  and  $G1$  parameters in the neck puck material model under lateral loading conditions was shown to dramatically improve the predictive response of the head-neck complex in this loading orientation (Figure 7.2-4).  $G0$  and  $G1$  parameters were increased, raising the overall stiffness of the neck pucks under bending (Table 7.2-3). These changes led to the most significant improvement in head rotational response, particularly the lower energy impact, in which the FEM had previously shown the poorest correlation with test results. The upper neck z force exhibited an improvement in prediction of peak load at lower energy. Updates did not reduce upper neck z force accuracy, which was predicted at higher energies in the original model. Reduction in noise exhibited from this channel was the result of the updated element formulation.

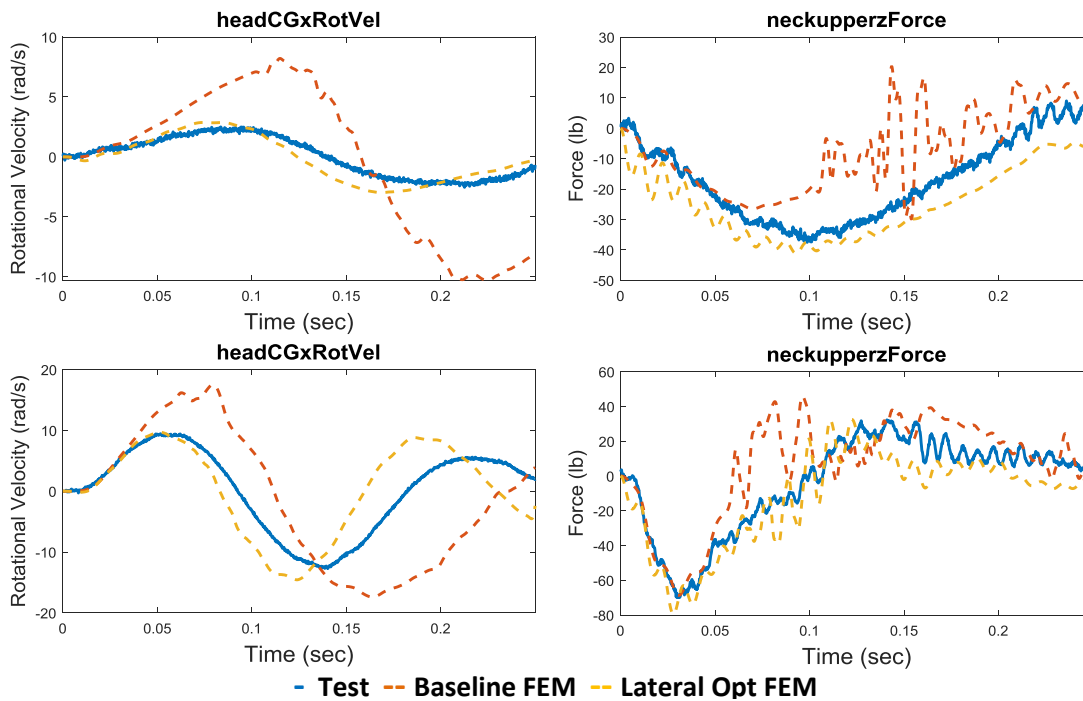


**Figure 7.2-4. Correlation Comparison between Baseline and Lateral Optimized FEM under Lateral Loading: 6 g–100 ms (top) and 12 g–100 ms (right)**

**Table 7.2-3. Optimized Parameters—Lateral Optimization**

Material Parameter	Baseline FEM	Lateral Opt
Short-term shear modulus, $G0$ , [psi]	6.67E2	1.16E3
Long-term shear modulus, $G1$ , [psi]	1.45E2	5.80E2

The second optimization, which included  $G0$ ,  $G1$ , and  $\beta$  under rearward loading improved the phasing of head rotational response in the optimized direction (Figure 7.2-5).  $G0$  was increased in this optimization, while  $\beta$  was reduced and  $G1$  was returned to its original value (Table 7.2-4). Though phasing improved in this optimization, the correlation of peak response, particularly in

the higher energy impact, was diminished. The optimization was unable to converge on a solution that improved this phase while maintaining the shape and peak response prediction by the FEM.

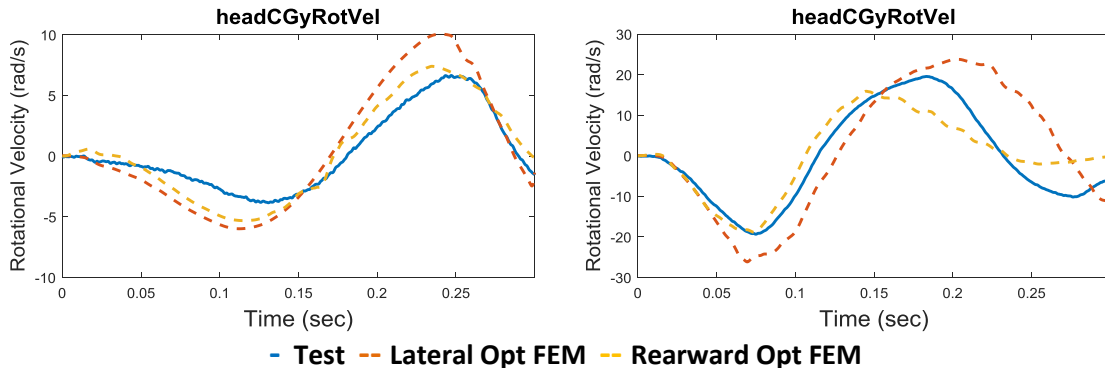


**Figure 7.2-5. Correlation Comparison between Lateral and Rearward Optimized FEM under Rearward Loading: 6 g–100 ms (left) and 16 g–50 ms (right)**

**Table 7.2-4. Optimized Parameters—Rearward Optimization**

Material Parameter	Baseline FEM	Lateral Opt	Rearward Opt
Short term shear modulus, $G_0$ , [psi]	6.67E2	1.16E3	1.31E3
Long term shear modulus, $G_l$ , [psi]	1.45E2	5.80E2	1.45E2
Decay constant, $\beta$	0.11	Not Optimized (0.11)	0.07

The manual optimization led to a change in  $G_0$ ,  $G_l$ , and  $\beta$  parameters, bringing them closer to the original optimization (Table 7.2-5). Phasing of head rotational response in the rearward and lateral impact directions improved (Figure 7.2-6). Phase was prioritized over magnitude in this optimization, as magnitude discrepancies can be accounted for through model uncertainty factors applied to the predicted output. A tradeoff in peak value correlation between the low- and high-energy impacts was required. Compared with the previous optimization, the manual optimization improved prediction of peak rotation throughout simulation in the 12 and 16 g cases, while slightly increasing the overprediction in the 6 g cases. This tradeoff was made to improve the predictive capability at impact energies most critical to defining injury risk. This improved correlation with impact energy was consistent with the small and medium male ATD FEMs. The calibration of the  $G_0$  and  $G_l$  parameters doubled their original value. This increase was considered reasonable given the variability in rubber stiffness values associated with various durometers. It is difficult to further assess the practicality of this change, as the rubber material approximated with these parameters is unknown.

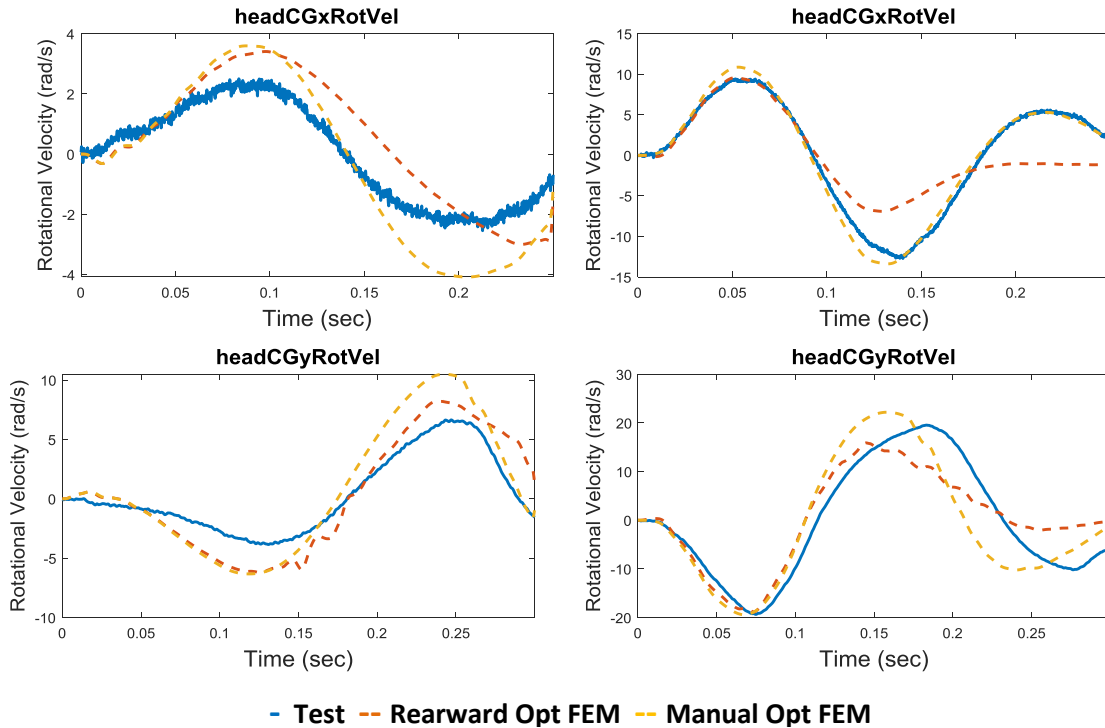


**Figure 7.2-6. Correlation Comparison between Rearward and Manual Optimized FEM under Lateral: 6 g–100 ms (top left) and 12 g–50 ms (top right) and Rearward Loading: 6 g–100 ms (bottom left) and 16 g–50 ms (bottom right)**

**Table 7.2-5. Optimized Parameters—Manual Optimization**

Material Parameter	Baseline FEM	Lateral Opt	Rearward Opt	Manual Opt
Short term shear modulus, $G_0$ , [psi]	6.67E2	1.16E3	1.31E3	1.15E3
Long term shear modulus, $G_l$ , [psi]	1.45E2	5.80E2	1.45E2	3.63E2
Decay constant, $\beta$	0.11	Not Optimized (0.11)	0.07	0.116

### 7.3 Verification of Large Male ATD FEM Correlation Improvement

The effectiveness of the material calibration was first verified through simulation of frontal impact tests to ensure improvements were robust for impact orientations and energy levels not directly used as part of the optimization. These verification tests included 6 g and 16 g peak acceleration at 100 and 50 ms rise time with a head-neck tilted 40°, and an 8 g peak acceleration at 50 ms rise time with the head-neck tilted 20° to the loading direction. Results indicated the improvements made to the model were valid in the frontal impact direction, where the response improved significantly in all impact energy levels with the updated FEM (Figure 7.3-1). The level of improvement at the 8 g/20° condition was comparable to or better with the other conditions.

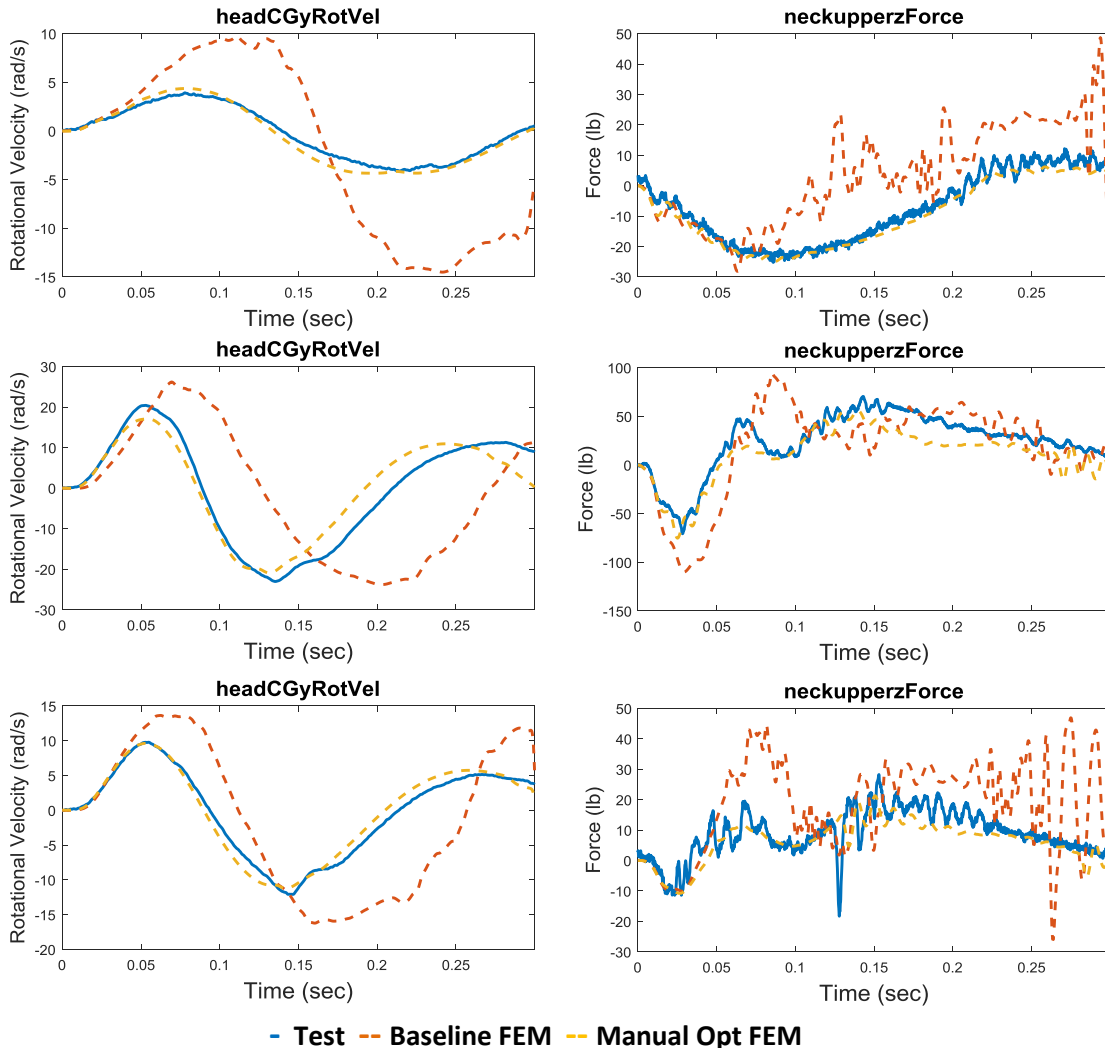


**Figure 7.3-1. Verification of Material Calibration under Frontal Loading: 6 g–100 ms (top), 16 g–50 ms (middle), 8 g–50 ms at 20° (bottom)**

A second set of verification simulations was performed to ensure that neglecting the preload and neck cable tension to more efficiently perform the optimization did not have a negative effect on the final FEM model’s ability to accurately predict the ATD response. The lateral and rearward impact cases used in optimization were re-run using the full boundary condition setup, including the 250-millisecond (ms) preload phase and neck cable tension. These are the boundary conditions the model is typically simulated within, considered the most realistic method for capturing the physical test conditions. Results indicate minor differences between the simplified and full boundary condition setup (Figure 7.3-2). The full boundary condition setup improved peak prediction in the lower energy impacts, and had no observed effect at higher energy impacts in the lateral and rear impact conditions. Based on these results, the assessment team concluded that the updated FEM was valid for use in the full boundary condition simulation setup.

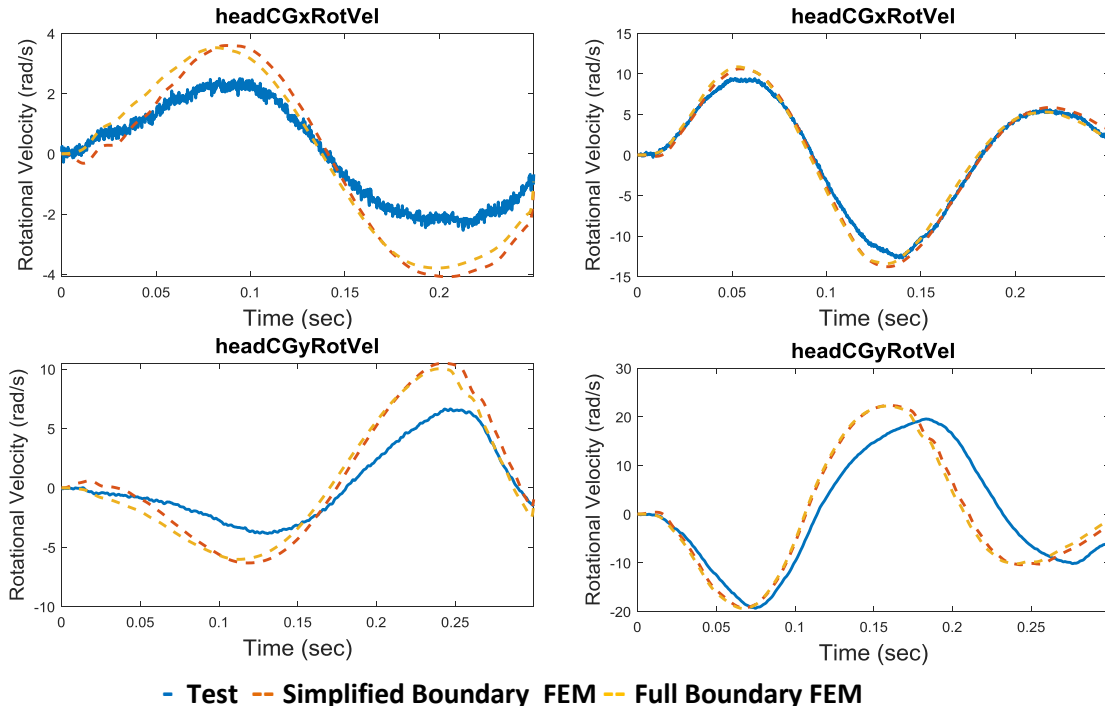


**Figure 7.3-2. Verification of Material Calibration with Full Boundary Conditions Implementation under Lateral: 6 g–100 ms (top left) and 12 g–50 ms (top right) and Rearward Loading: 6 g–100 ms (bottom left) and 16 g–50 ms (bottom right)**

The improvements to the large male ATD head-neck complex FEM were verified quantitatively by simulating the FEM in all conditions tested in the isolated head-neck test series. The accuracy of each predictive response was measured using the ISO/TR 16250:2013 curve rating methodology [ref. 5], and those ratings compared to the original FEM. The ISO/TR rating methodology scores the correlation between two curves on a scale of 0 to 1, where 0 indicates no correlation and 1 an exact match. These scores are calculated based on the evaluation of magnitude, phase, and slope between the two curves. Tabulated scores for each response can be found in Tables 7.3-1 and 7.3-2. Comparison plots of each response are provided in Appendix A. For each test, only the channels exercised in the direction of impact were evaluated, thus in frontal impacts no lateral response channels were evaluated, and in the combined frontal- and rear-lateral cases all channels were evaluated.

The NESC recommended a computed ISO/TR 16250:2013 score of at least 0.5 for a response to be considered a valid prediction of ATD response [ref. 6]. This threshold was chosen based on subject matter experts' qualitative assessment of a set of ATD FEM correlation plots compared to ISO/TR 16250 scores for the same correlations. ISO scores of 0.5 or greater were found to correspond with the correlations deemed acceptable. The threshold, developed in a previous NESC study, did not include any of the data used in this assessment. Of the 199 responses evaluated in this study, more than 50% (108 responses) failed these criteria with the original FEM. With the updated FEM, only 2.5% failed (5 responses). Furthermore, of the responses failing the 0.5 threshold, all did so with value of 0.45 or greater. These results indicate a successful correlation improvement of the large male ATD FEM, which is robust to impact energy and orientation within the expected load conditions for current spaceflight landing analysis.

**Table 7.3-1. ISO/TR 16250:2013 Rating for Each Response Predicted by Baseline FEM**

	Head Gx	Head Gy	Head Gz	Head Gx Rot Vel	Head Gy Rot Vel	Neck Upper Fx	Neck Upper Fy	Neck Upper Fz	Neck Upper Mx	Neck Upper My	Nij
Frontal 6g 100ms	0.50		0.34		0.25	0.50		0.25		0.37	0.31
Frontal 8g 50ms	0.54		0.42		0.29	0.54		0.53		0.44	0.35
Frontal 10g 100ms	0.71		0.35		0.31	0.68		0.33		0.56	0.41
Frontal 12g 100ms	0.79		0.38		0.35	0.75		0.33		0.62	0.51
Frontal 12g 50ms	0.65		0.42		0.38	0.65		0.59		0.56	0.49
Frontal 16g 50ms	0.63		0.56		0.50	0.64		0.63		0.60	0.52
Lateral 6g 100ms		0.58	0.40	0.24			0.55	0.41	0.47		0.54
Lateral 8g 50ms		0.46	0.61	0.26			0.43	0.70	0.38		0.58
Lateral 10g 100ms		0.62	0.28	0.27			0.58	0.30	0.52		0.600
Lateral 10g 50ms		0.48	0.56	0.28			0.46	0.67	0.41		0.64
Lateral 12g 100ms		0.52	0.59	0.26			0.49	0.62	0.47		0.610
Lateral 12g 50ms		0.47	0.58	0.29			0.43	0.65	0.42		0.53
Rearward 6g 100ms	0.50		0.32		0.29	0.42		0.34		0.31	0.34
Rearward 8g 100ms	0.70		0.38		0.35	0.59		0.41		0.36	0.43
Rearward 8g 50ms	0.49		0.57		0.27	0.43		0.65		0.31	0.47
Rearward 10g 100ms	0.72		0.39		0.36	0.63		0.41		0.47	0.61
Rearward 12g 100ms	0.56		0.62		0.33	0.53		0.69		0.47	0.68
Rearward 12g 50ms	0.72		0.42		0.44	0.67		0.41		0.57	0.74
Rearward 16g 50ms	0.55		0.71		0.46	0.53		0.72		0.53	0.79
Rear-Lat 8g 50ms	0.40	0.50	0.67	0.22	0.27	0.38	0.48	0.71	0.41	0.32	0.57
Rear-Lat 12g 50ms	0.43	0.57	0.64	0.31	0.30	0.41	0.54	0.66	0.46	0.40	0.68
Rear-Lat 16g 50ms	0.49	0.60	0.70	0.33	0.37	0.46	0.56	0.69	0.51	0.46	0.77
Front-Lat 8g 50ms	0.57	0.53	0.47	0.26	0.30	0.56	0.48	0.63	0.43	0.50	0.49
Front-Lat 12g 50ms	0.69	0.48	0.46	0.28	0.48	0.67	0.45	0.56	0.38	0.54	0.48
Front-Lat 16g 50ms	0.70	0.50	0.59	0.31	0.56	0.70	0.47	0.66	0.45	0.60	0.59

**Table 7.3-2. ISO/TR 16250:2013 Rating for Each Response Predicted by Updated FEM**

	Head Gx	Head Gy	Head Gz	Head Gx Rot Vel	Head Gy Rot Vel	Neck Upper Fx	Neck Upper Fy	Neck Upper Fz	Neck Upper Mx	Neck Upper My	Nij
Frontal 6g 100ms	0.98		0.84		0.78	0.96		0.89		0.93	0.94
Frontal 8g 50ms	0.93		0.78		0.88	0.95		0.80		0.89	0.90
Frontal 10g 100ms	0.94		0.72		0.84	0.95		0.73		0.86	0.86
Frontal 12g 100ms	0.87		0.63		0.72	0.85		0.73		0.75	0.82
Frontal 12g 50ms	0.78		0.65		0.60	0.60		0.67		0.69	0.80
Frontal 16g 50ms	0.72		0.68		0.56	0.71		0.73		0.64	0.75
Lateral 6g 100ms		0.94	0.91	0.45			0.88	0.89	0.95		0.95
Lateral 8g 50ms		0.90	0.94	0.69			0.83	0.87	0.83		0.90
Lateral 10g 100ms		0.96	0.88	0.80			0.92	0.83	0.93		0.960
Lateral 10g 50ms		0.96	0.91	0.92			0.93	0.85	0.91		0.93
Lateral 12g 100ms		0.93	0.86	0.81			0.90	0.81	0.89		0.93
Lateral 12g 50ms		0.96	0.91	0.91			0.92	0.86	0.92		0.89
Rearward 6g 100ms	0.77		0.55		0.47	0.71		0.69		0.56	0.61
Rearward 8g 100ms	0.58		0.55		0.56	0.50		0.68		0.47	0.61
Rearward 8g 50ms	0.80		0.77		0.63	0.68		0.84		0.62	0.72
Rearward 10g 100ms	0.56		0.56		0.56	0.48		0.66		0.49	0.65
Rearward 12g 100ms	0.63		0.72		0.58	0.50		0.78		0.53	0.71
Rearward 12g 50ms	0.64		0.62		0.61	0.56		0.66		0.58	0.75
Rearward 16g 50ms	0.66		0.78		0.65	0.56		0.81		0.64	0.81
Rear-Lat 8g 50ms	0.86	0.88	0.88	0.65	0.75	0.86	0.84	0.89	0.81	0.78	0.90
Rear-Lat 12g 50ms	0.72	0.87	0.83	0.76	0.69	0.72	0.86	0.88	0.82	0.68	0.87
Rear-Lat 16g 50ms	0.71	0.89	0.84	0.77	0.65	0.67	0.86	0.88	0.86	0.68	0.91
Front-Lat 8g 50ms	0.96	0.93	0.89	0.74	0.94	0.98	0.81	0.89	0.84	0.94	0.93
Front-Lat 12g 50ms	0.81	0.96	0.77	0.84	0.68	0.84	0.82	0.76	0.90	0.78	0.90
Front-Lat 16g 50ms	0.89	0.74	0.73	0.61	0.74	0.89	0.78	0.72	0.71	0.88	0.82

Modeling and simulation code verification was performed to ensure the FEM response was robust to LS-DYNA implementation methodology. All verification simulations were performed on a Windows platform to ensure improvements were not specific to the Linux platform they were developed in. No differences were observed between matching runs on the two platforms. A single case was simulated in both single and double precision as well as using LS-DYNA SMP Version R10.1.0 and Version R8.0.0 to ensure results were robust to version and precision used in the FEM simulation. Perfect unity was shown between results in these test cases, verifying that the FEM was robust to computational implementation methodology.

The updated head-neck complex was re-integrated into the LSTC Hybrid III large male FEM version 3.03\_Beta [ref. 1]. All parts in the head-neck complex (lower neck attachment bracket to head skin) were replaced (Figure 7.3-4). The updated full ATD FEM has been simulated in a variety of crash impact simulations. Results have verified the stability of the updated parts and their re-integration within the full ATD FEM.

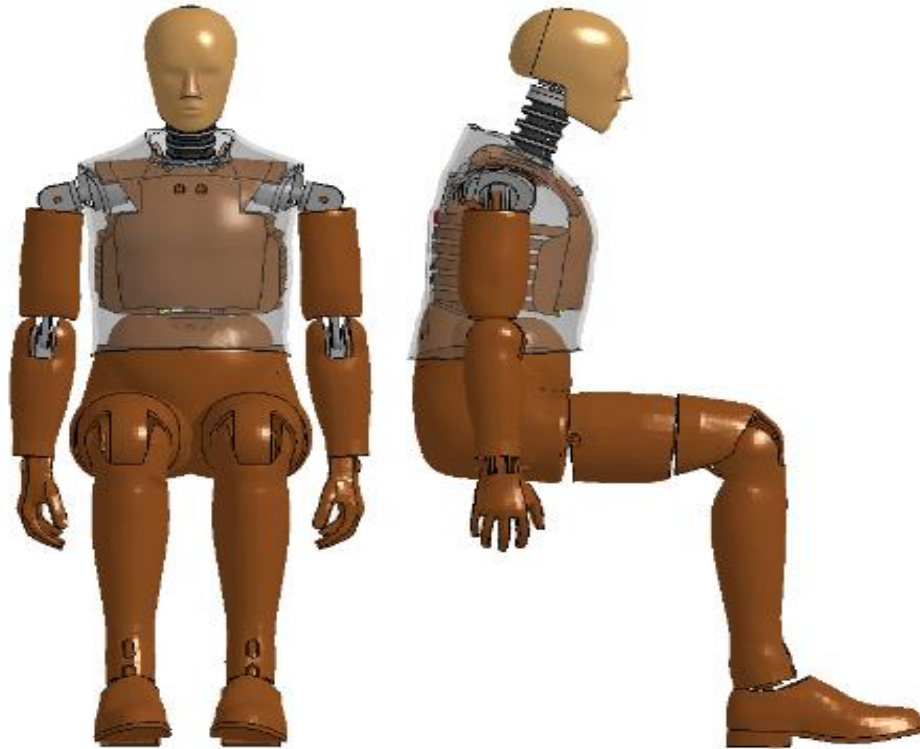


***Figure 7.3-3. Updated Head-Neck Complex Integrated into Hybrid III Large Male FEM***

Throughout the correlation effort, the NESC assessment team met biweekly with the FEM developer, LSTC, to ensure changes were implemented appropriately. The updates to the head-neck FEM have been provided to LSTC, which will run the updated model through a more expansive set of impact conditions to assess the viability of these improvements in a broader range of crash impact applications (e.g., automotive). Post-validation, these updates will be included in a new version of the LSTC Hybrid III large male ATD FEM to be publicly released with additional updates currently in work.

## **8.0 Findings and Observations**

### **8.1 Findings**

- F-1.** The physical dimensions of the large male ATD neck pucks were the same as the medium male ATD, but included additional spacers to increase neck length.
- F-2.** Neck geometry and neck material properties were identified as being different between the physical and FEM large male ATD.
- F-3.** Adding the spacer components found in the large male ATD to the medium male neck FEM generated a FEM geometrically accurate to the large male ATD.
- F-4.** The transient oscillations predicted by the FEM that were not observed in the test results were eliminated by changing the element formulation from the default constant stress solid formulation to fully integrated S/R solid.
- F-5.** Of the five material parameters used to define the viscoelastic material model of the neck puck parts, only the short-term shear modulus,  $G_0$ , the long-term shear modulus,  $G_I$ , and decay constant,  $\beta$ , were found to influence the correlation between the FEM predictions and the test data.
- F-6.** The original, unmodified large male ATD FEM correlation failed the minimum ISO criteria for over 50% of the response correlation comparisons.
- F-7.** The updated large male ATD FEM correlation passed the minimum ISO criteria for over 97% of the response correlation comparisons.
- F-8.** The updated large male ATD FEM was robust to impact energy levels and orientations not directly calibrated to.

### **8.2 Observations**

- O-1.** The Orion occupant protection team was receptive to the updates made to the large male ATD FEM.
- O-2.** Correlation was evaluated under accelerative loading conditions expected for current spacecraft; uncertainty remains in the predictive accuracy of the ATD FEM response when used outside of these impact conditions.

## **9.0 Alternative Viewpoint(s)**

No alternative viewpoints were identified during the course of this assessment by the NESC team.

## **10.0 Other Deliverables**

The updated large male ATD FEM and associated correlation results were electronically transferred to the Lockheed Martin lead crew injury analyst and Orion Crew Survival Suit crew injury analyst in support of Orion occupant protection analysis. These data and results were also provided to the original ATD FEM developer, LSTC.

## 11.0 Lessons Learned

No lessons learned were identified during the course of this assessment by the NESC team.

## 12.0 Recommendations for NASA Standards and Specifications

No recommendations were identified during the course of this assessment.

## 13.0 Definition of Terms

Finding	A relevant factual conclusion and/or issue that is within the assessment scope and that the team has rigorously based on data from their independent analyses, tests, inspections, and/or reviews of technical documentation.
Observation	A noteworthy fact, issue, and/or risk, which may not be directly within the assessment scope, but could generate a separate issue or concern if not addressed. Alternatively, an observation can be a positive acknowledgement of a Center/Program/Project/Organization's operational structure, tools, and/or support provided.
Recommendation	A proposed measurable stakeholder action directly supported by specific Finding(s) and/or Observation(s) that will correct or mitigate an identified issue or risk.

## 14.0 Acronyms and Nomenclature

ATD	anthropomorphic test device
CCP	Commercial Crew Program
CM	Crew Module
FEM	finite element model
$G_0$	short-term shear modulus
$G_I$	long-term shear modulus
$g$	unit of gravitational acceleration
in	inch
ISO/TR	International Organization for Standardization/Technical Report
lb	pound
LSTC	Livermore Software Technology Corporation
MPCV	Multi-Purpose Crew Vehicle
ms	milliseconds
NESC	NASA Engineering and Safety Center
NRB	NESC Review Board
OC	occipital condyle
psi	pounds per square inch
s	seconds
S/R	selectively reduced
$\beta$	decay constant

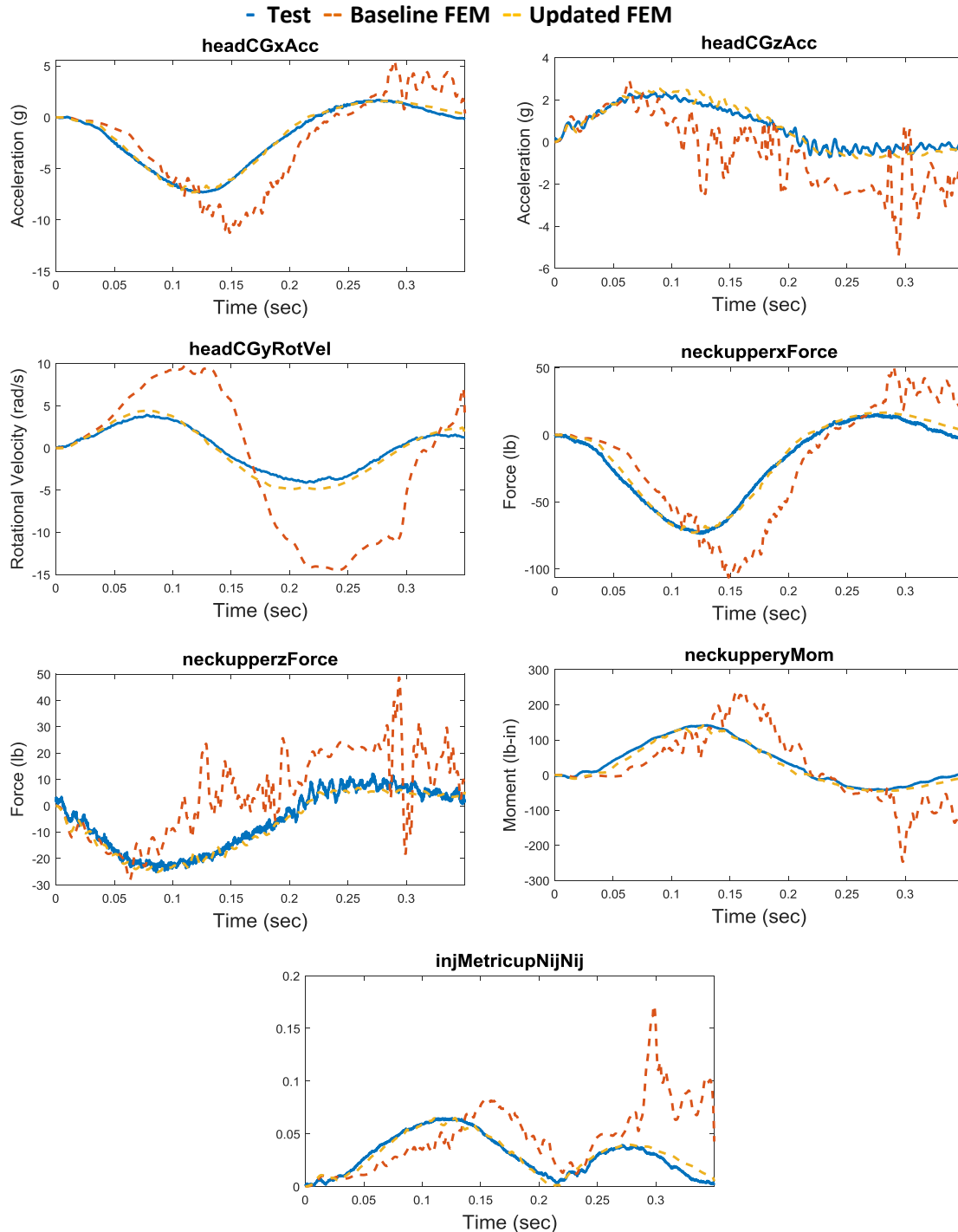
## 15.0 References

1. Guha, S. (2015). README.LSTC.H3\_95TH\_DETAILED\_Scaled.151214.V3.03\_BETA. LSTC Michigan.
2. Guha, S. (2014). LSTC\_NCAC Hybrid III 50th Dummy Positioning & Post-Processing. LSTC Michigan.
3. Humanetics. “Hybrid III 95th Large Male.” Retrieved 6/25/19, 2019, from <https://www.humaneticsatd.com/crash-test-dummies/frontal-impact/hiii-95m>.
4. Stander, N., et al. (2015). LS-OPT User’s Manual: A Design Optimization and Probabilistic Analysis Tool for the Engineering Analyst, LSTC.
5. International Organization for Standardization (2013). Road Vehicles—Objective Rating Metrics for Dynamic Systems.
6. NESC-RP-13-00876, Analysis of Anthropomorphic Test Device (ATD) Response for Proposed Orion Crew Impact Attenuation System (CIAS).

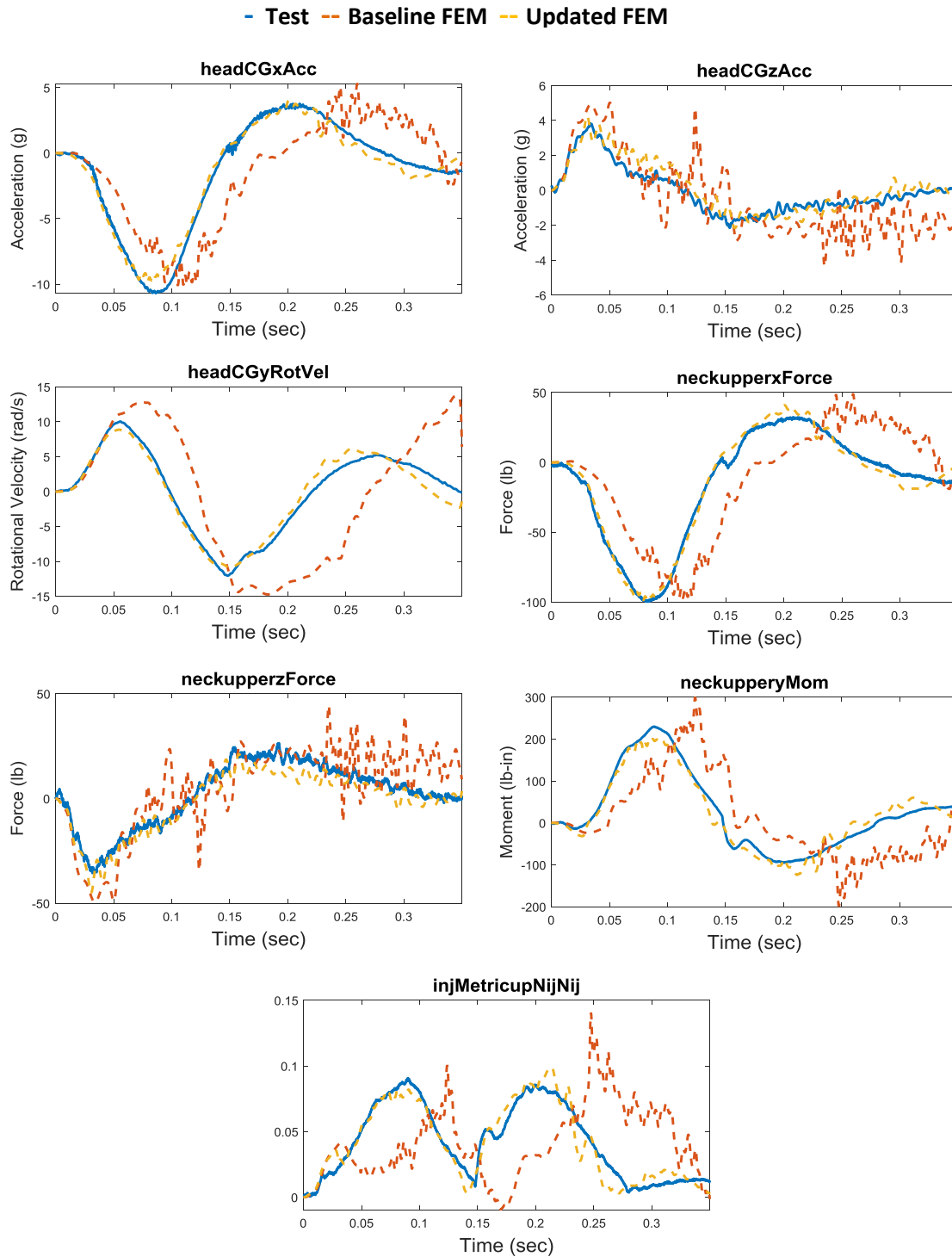
## Appendices

- A. Correlation Results of the Updated Large Male ATD Head-Neck FEM under Frontal, Rearward, Lateral, and Multi-Axis Loading

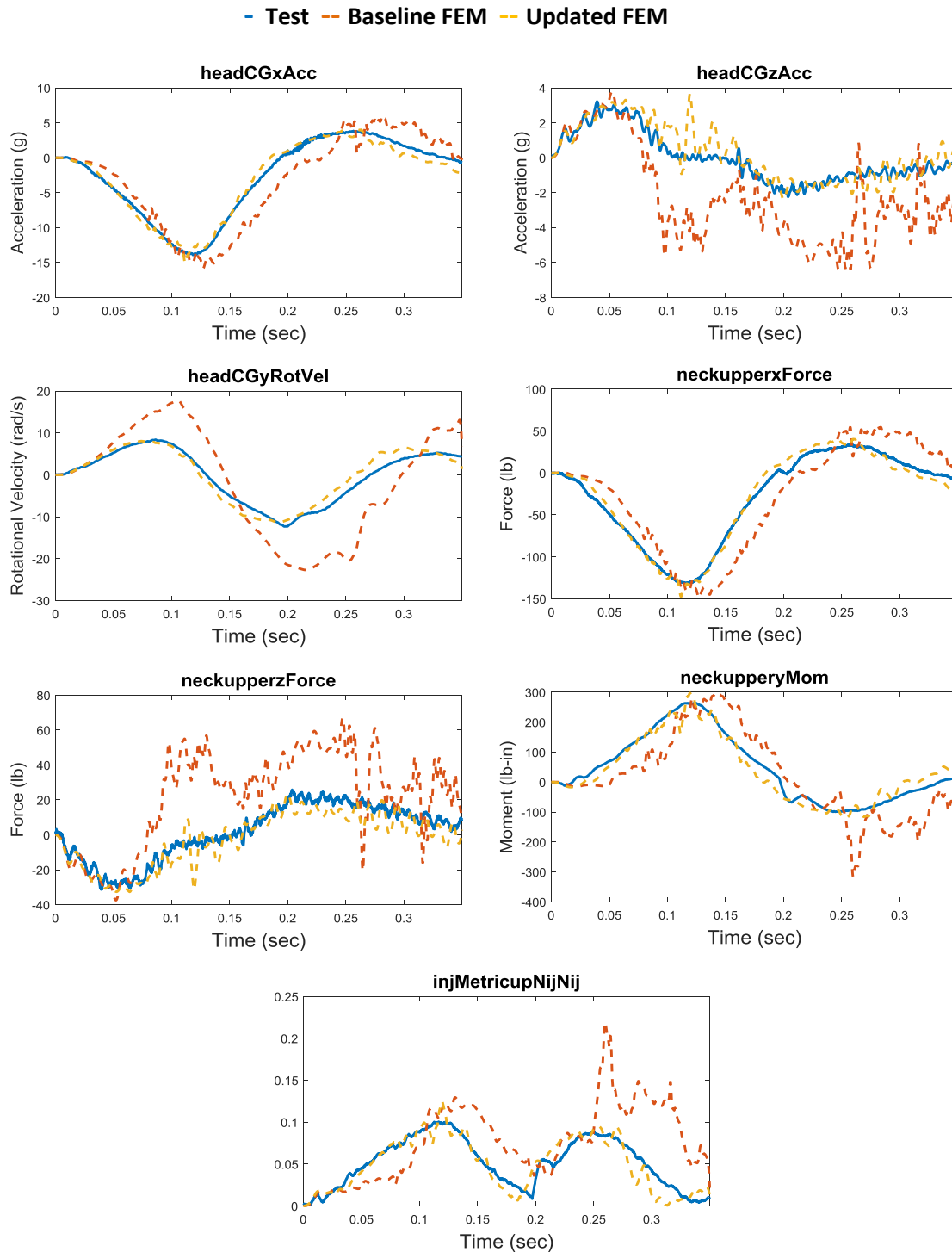
# Appendix A: Correlation Results of the Updated Large Male ATD Head-Neck FEM under Frontal, Rearward, Lateral, and Multi-Axis Loading



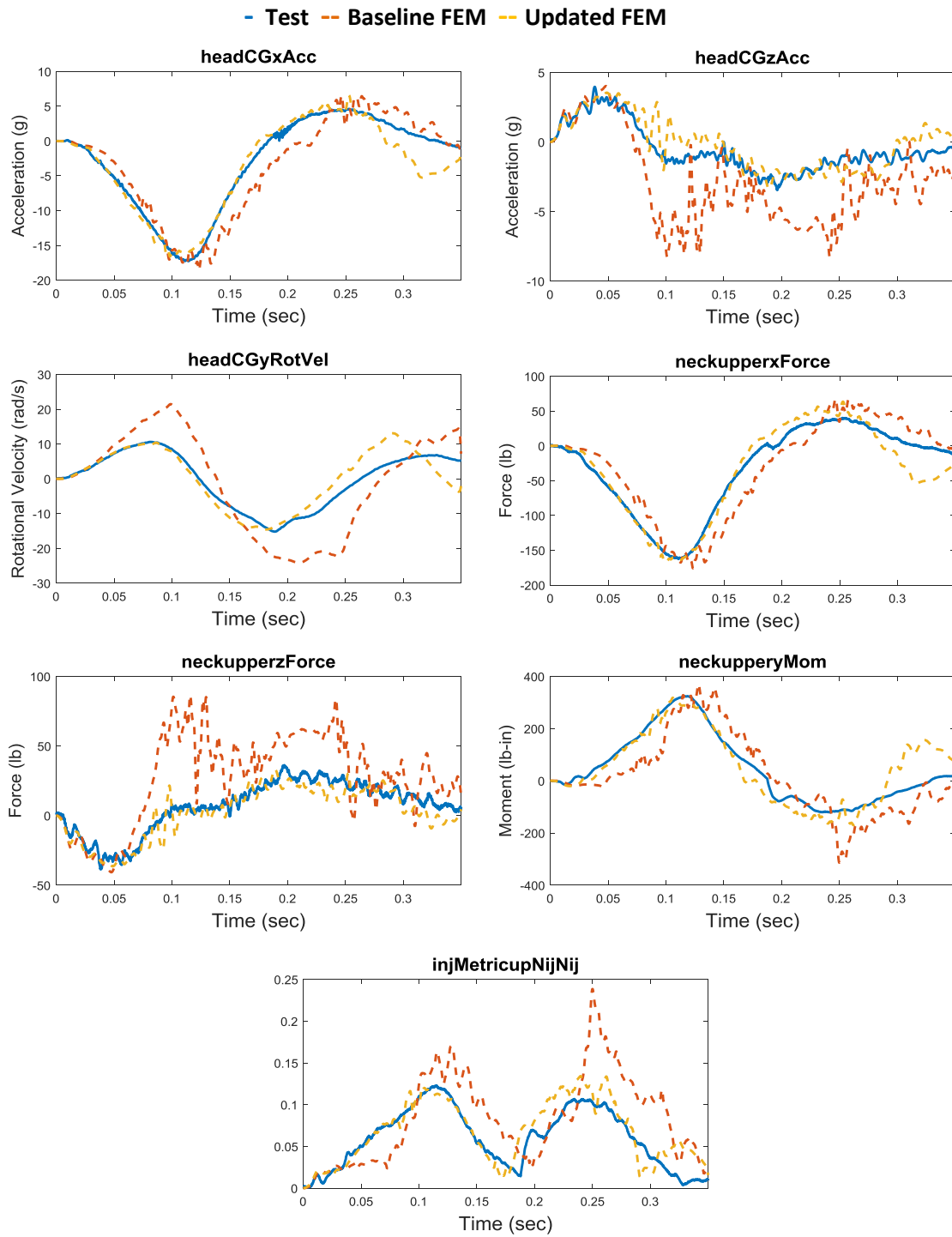
**Figure A-1. Test 9704: Frontal Impact 6-g 50ms**



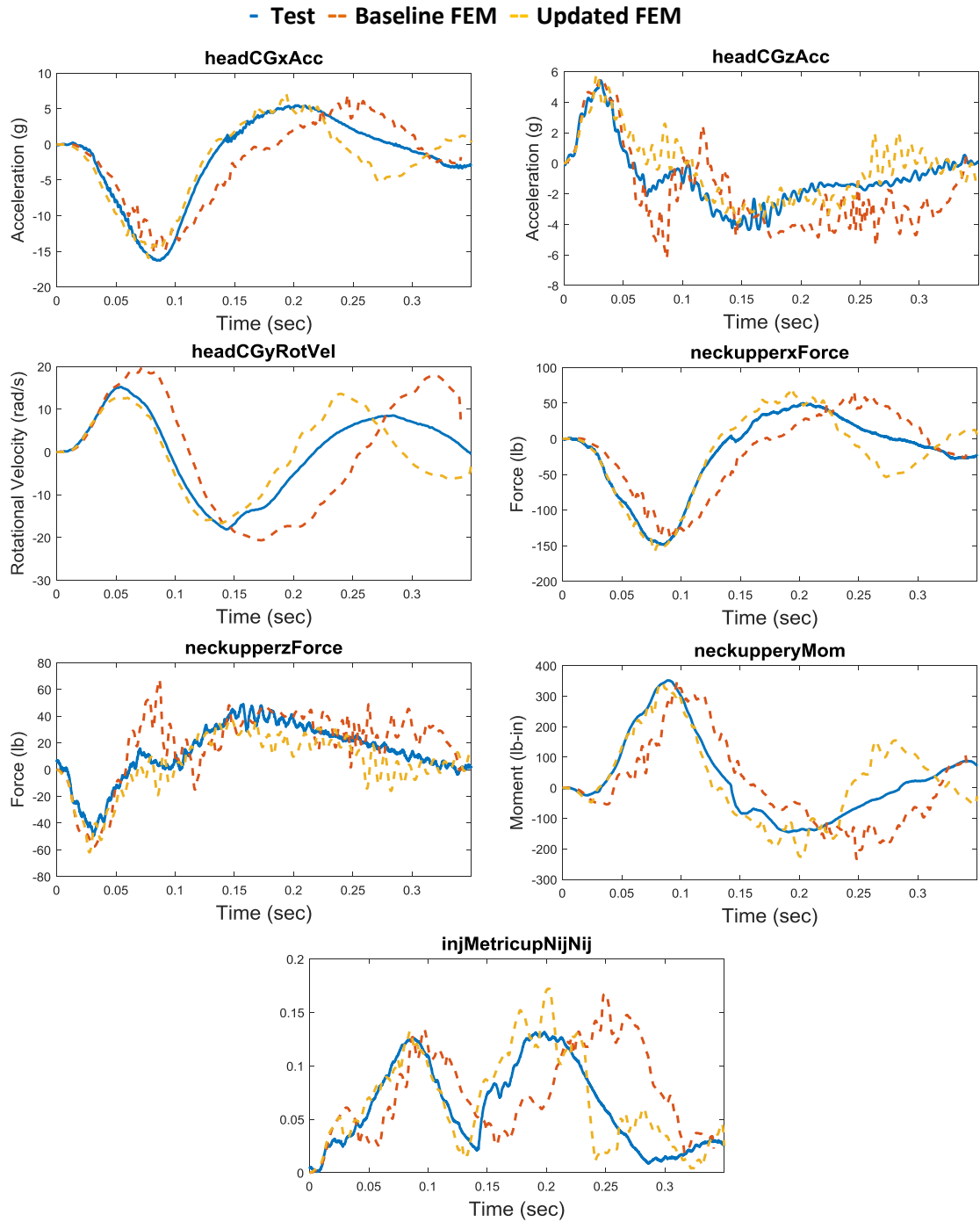
**Figure A2. Test 9740: Frontal Impact 8-g 50ms**



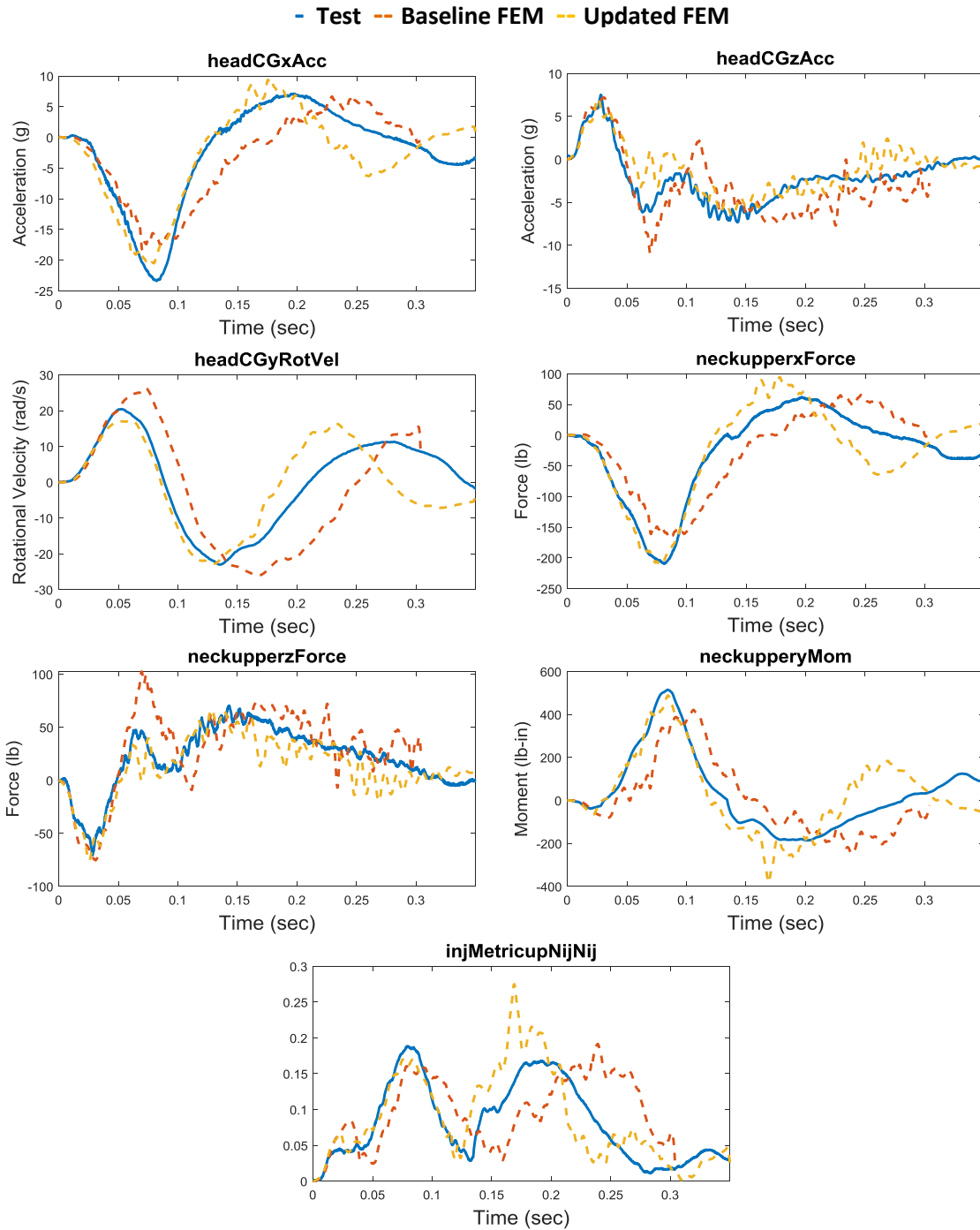
**Figure A3. Test 9708: Frontal Impact 10-g 100ms**



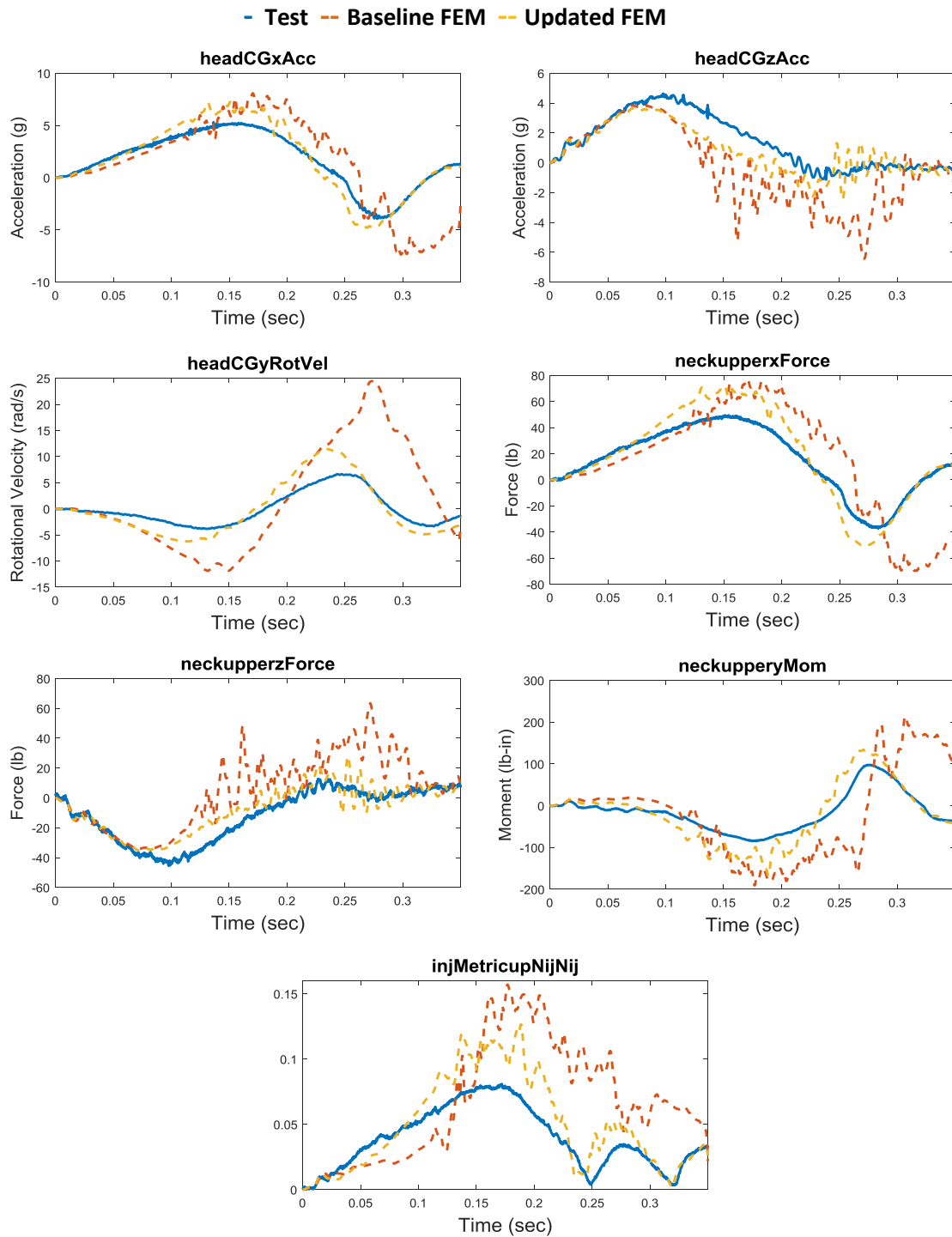
**Figure A4: Test 9713: Frontal Impact 12-g 100ms**



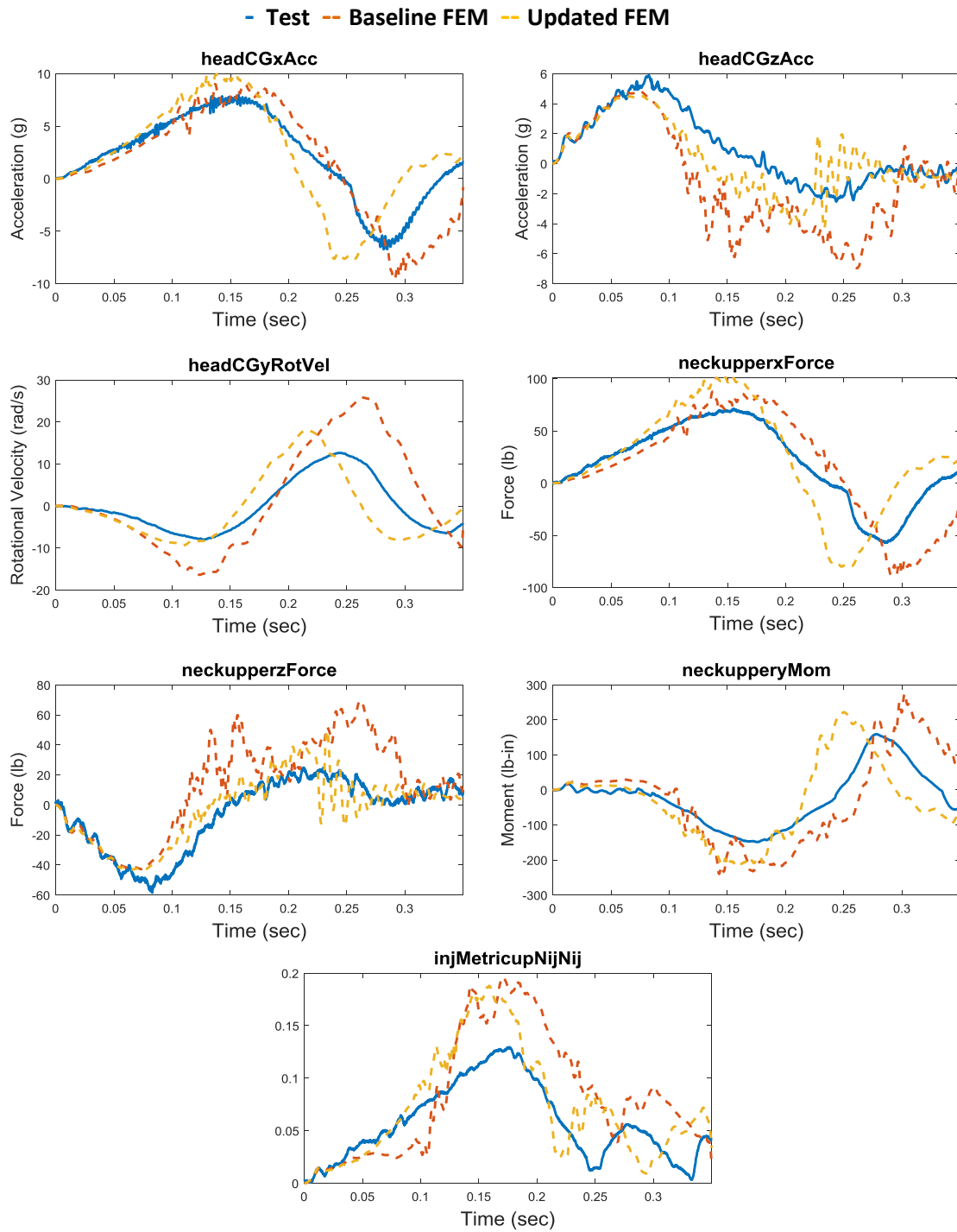
**Figure A5: Test 9741: Frontal Impact 12-g 50ms**



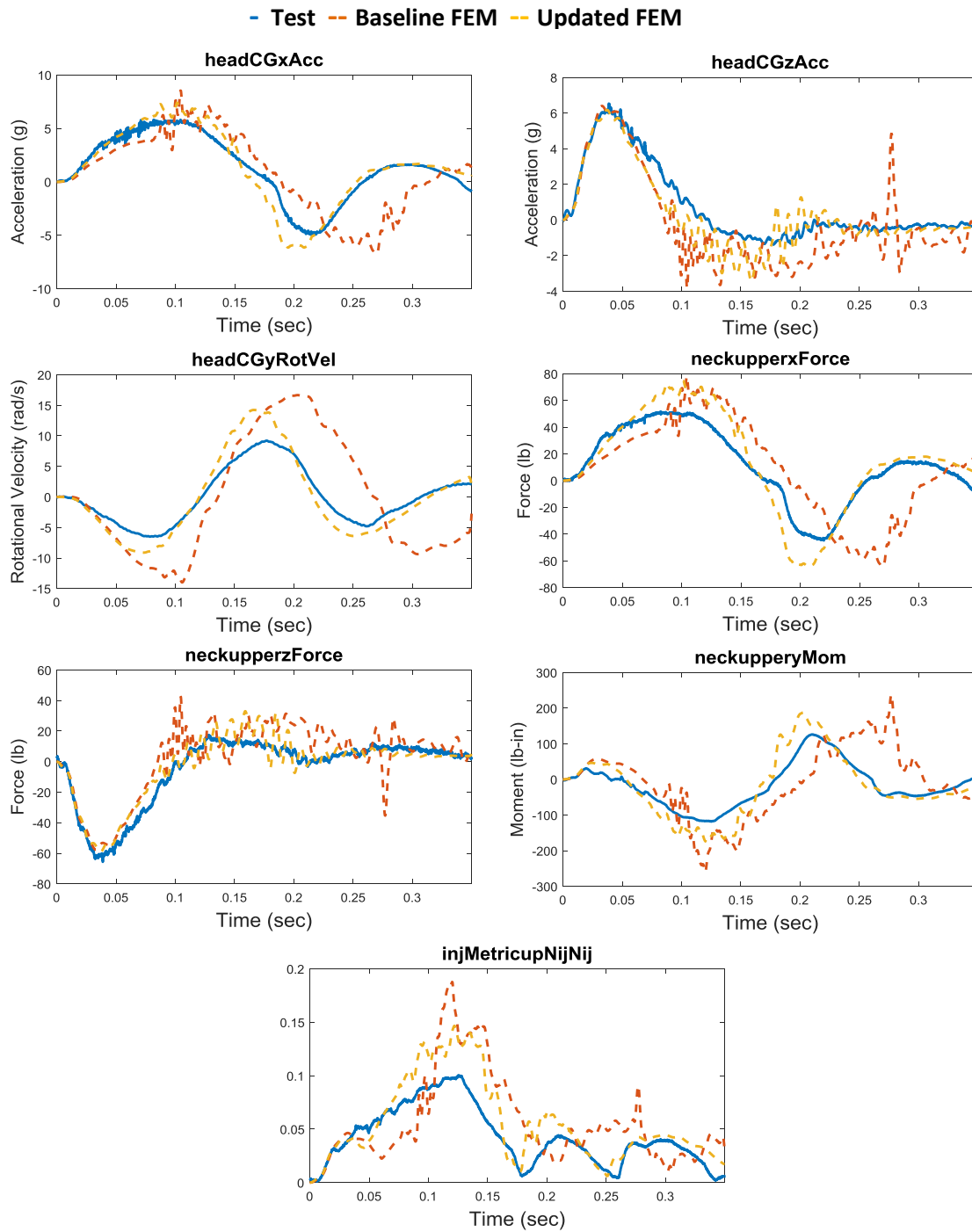
**Figure A6. Test 9742: Frontal Impact 16-g 50ms**



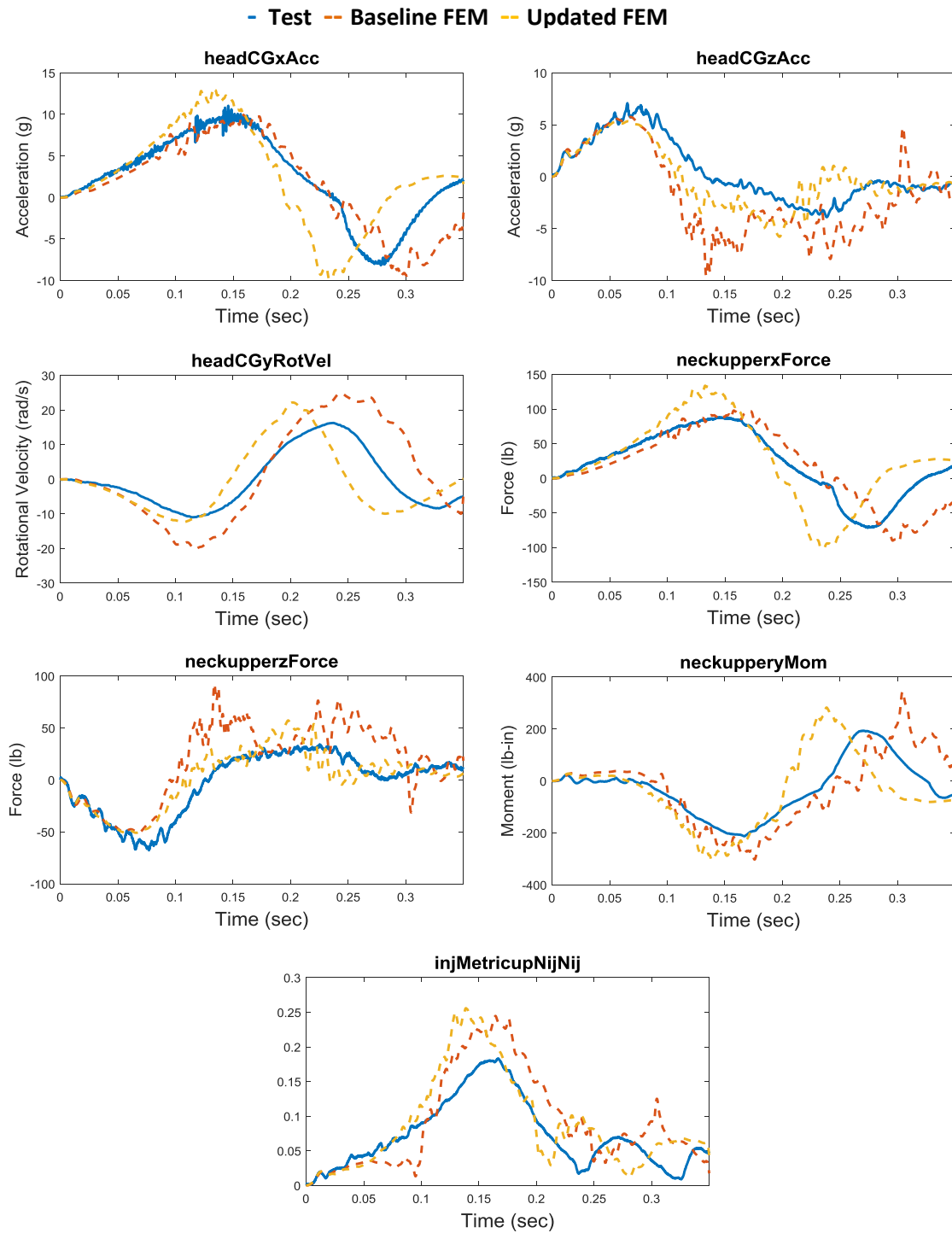
**Figure A7. Test 9702: Rearward Impact 6-g 100ms**



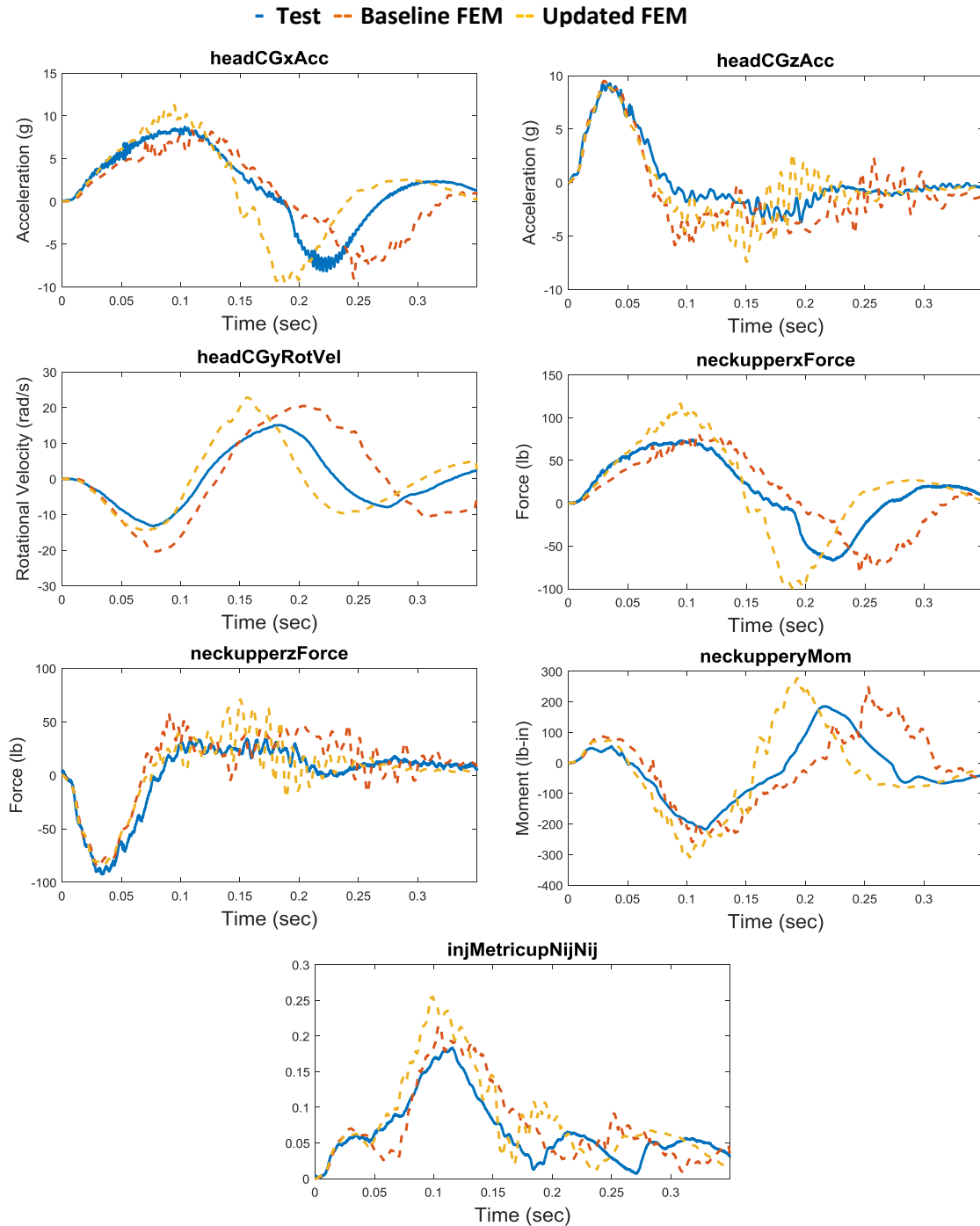
**Figure A8. Test 9712: Rearward Impact 8-g 100ms**



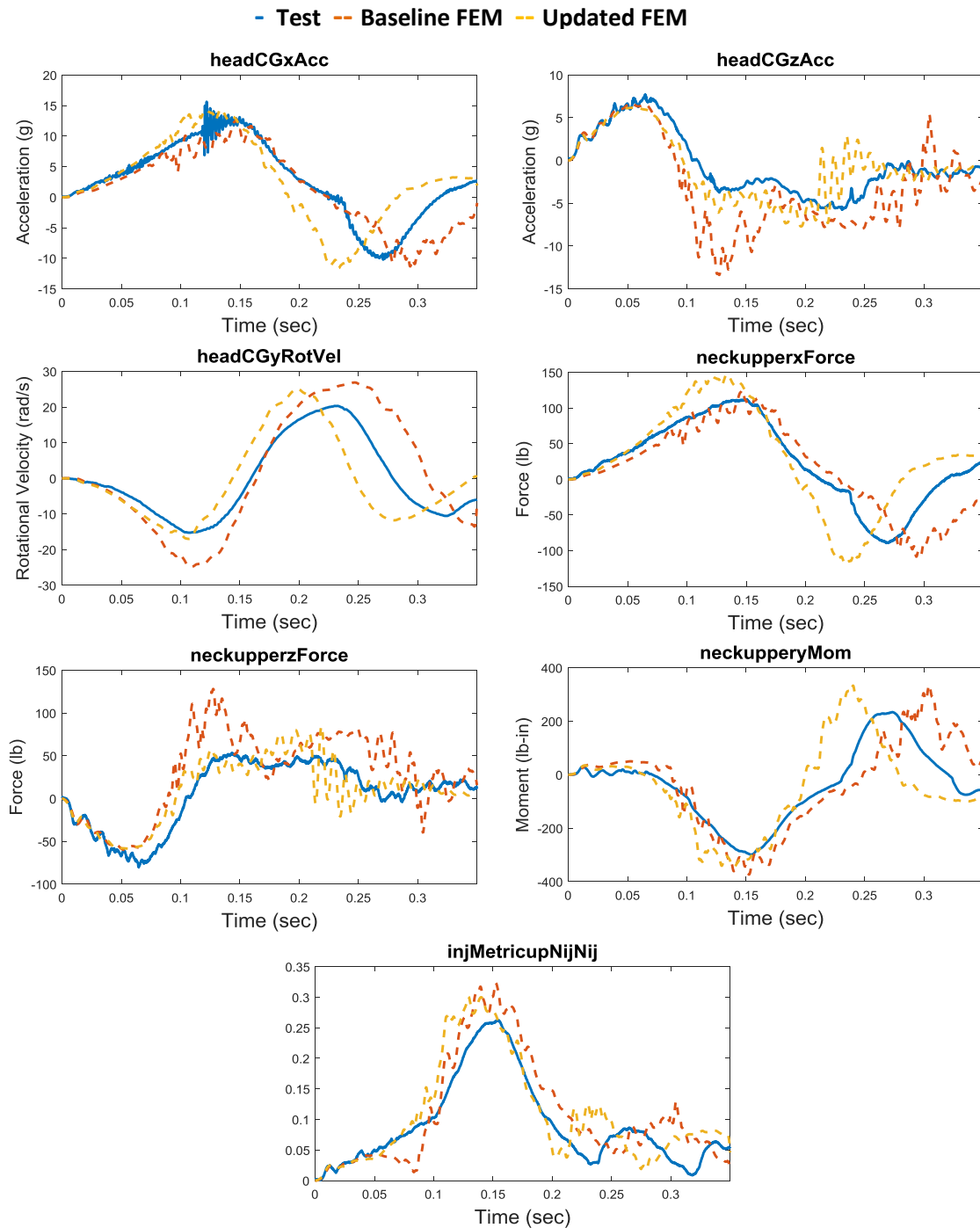
**Figure A9. Test 9734: Rearward Impact 8-g 50ms**



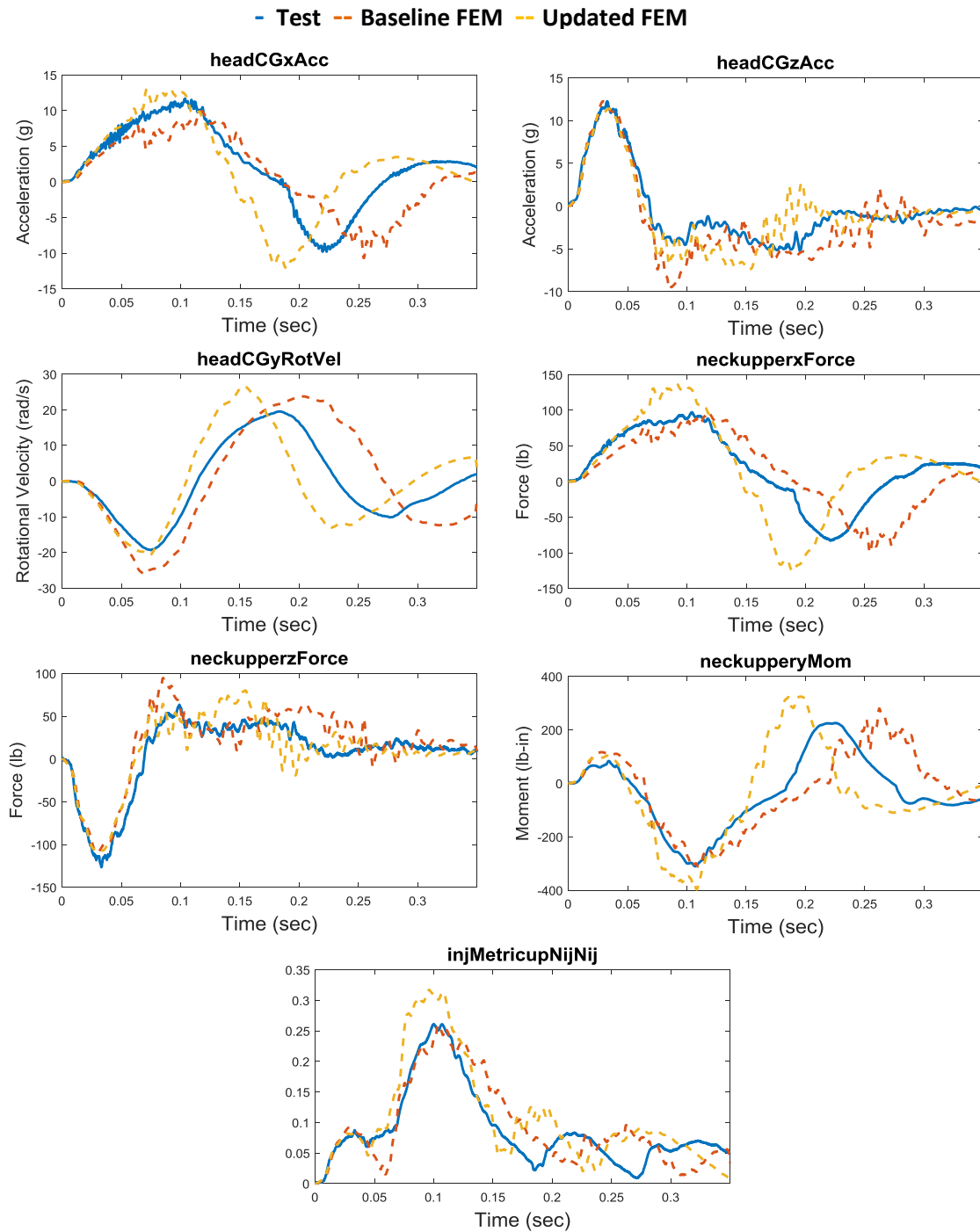
**Figure A10. Test 9706: Rearward Impact 10-g 100ms**



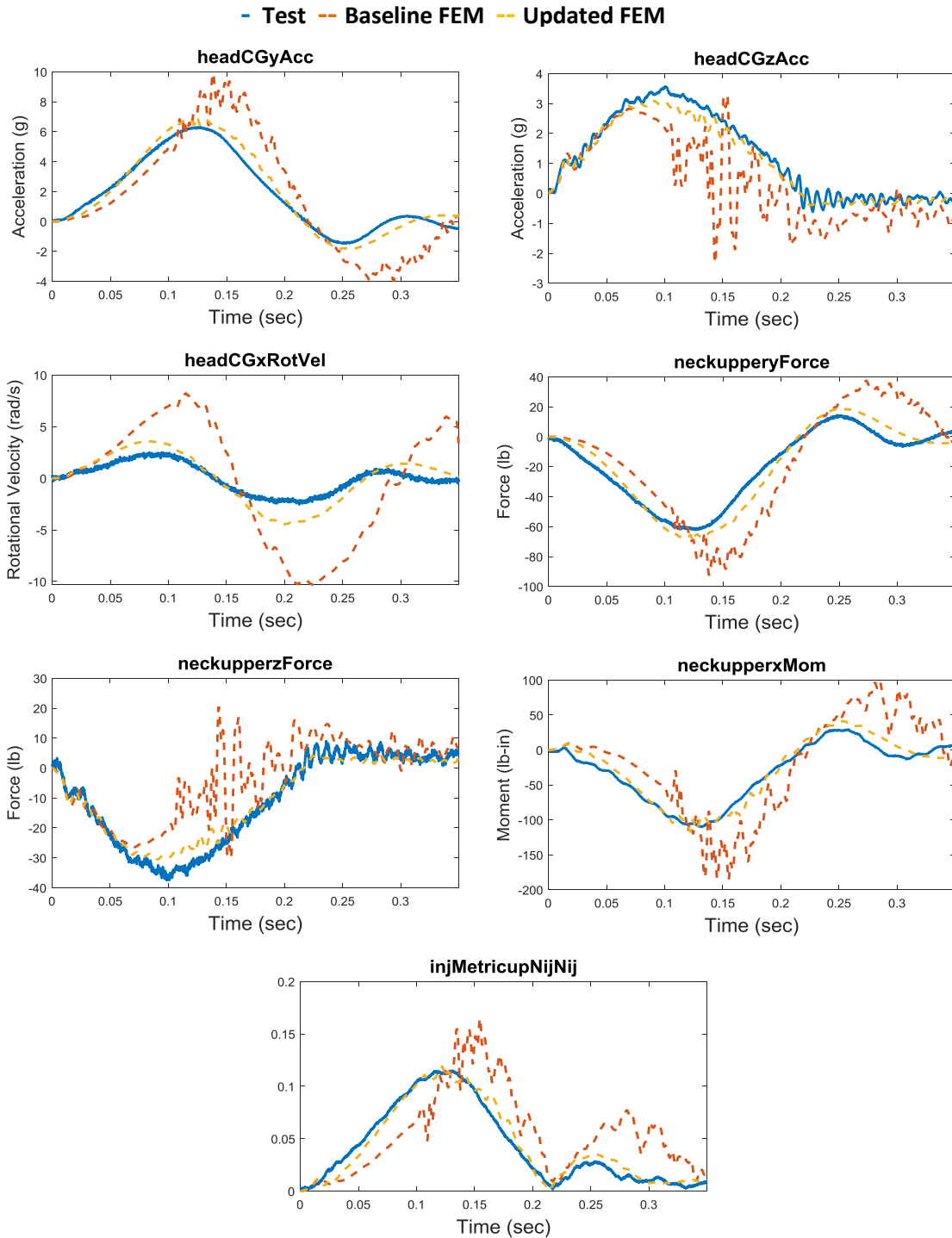
**Figure A11. Test 9735: Rearward Impact 12-g 50ms**



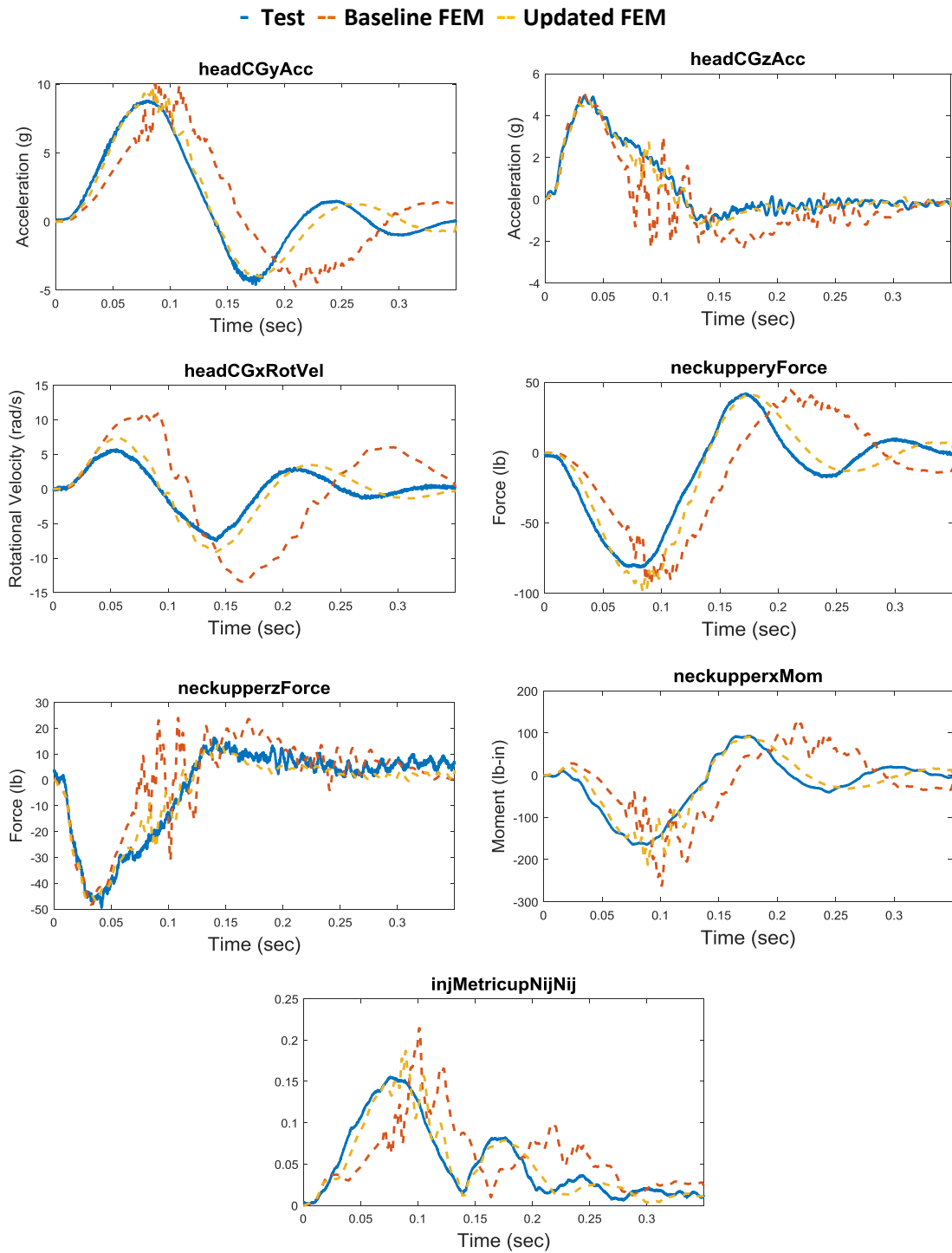
**Figure A12. Test 9711: Rearward Impact 12-g 100ms**



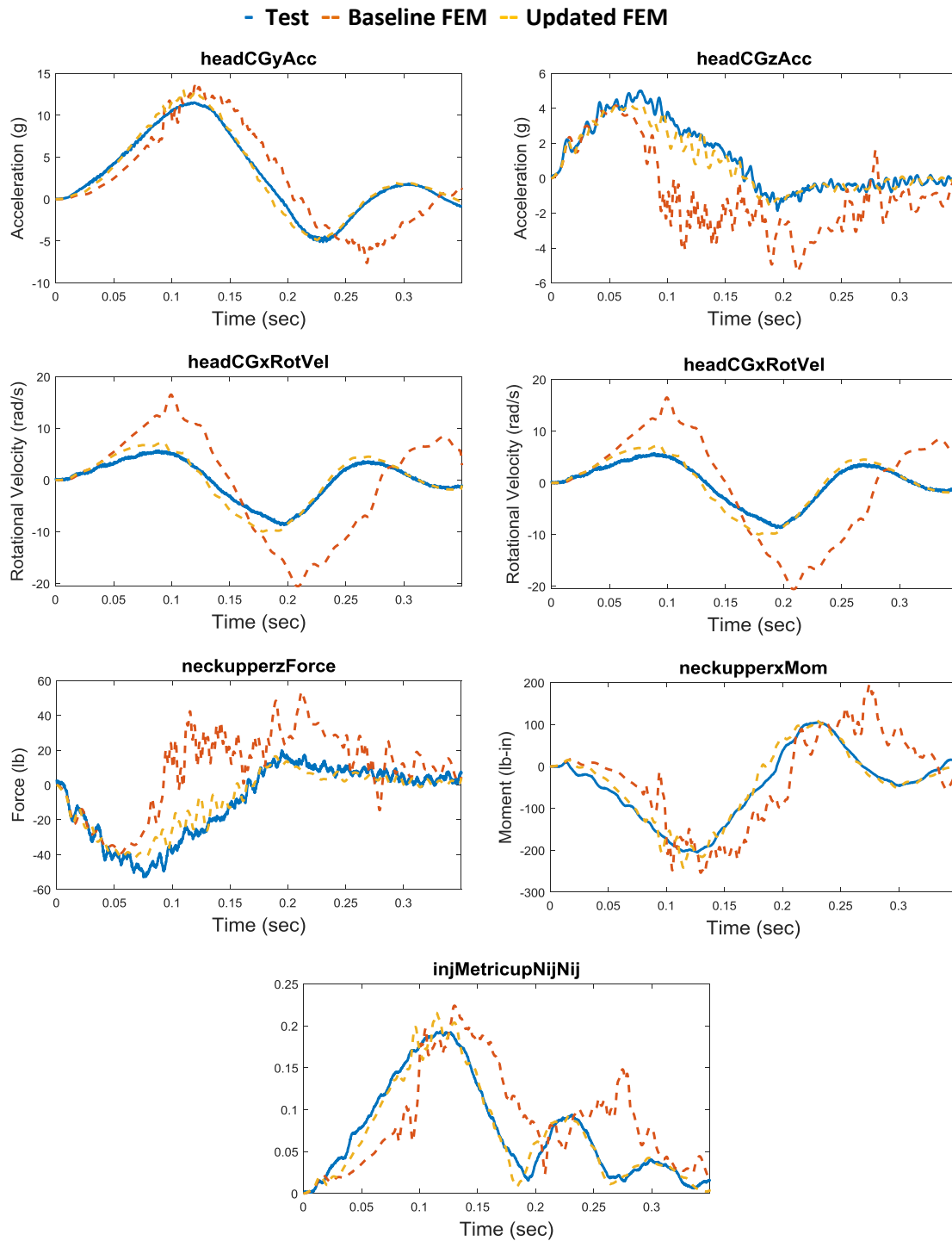
**Figure A13. Test 9736: Rearward Impact 16-g 50ms**



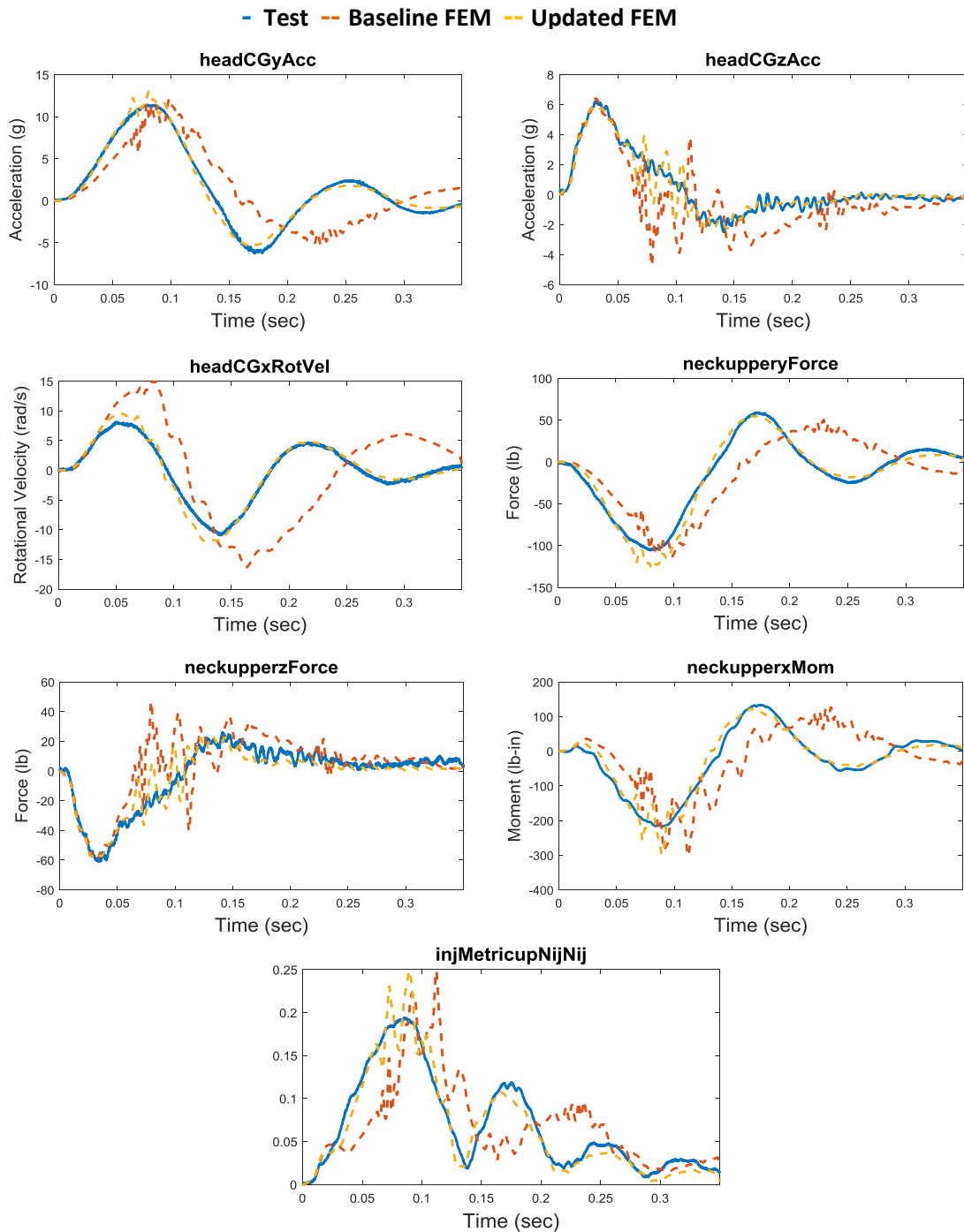
**Figure A14. Test 9703: Lateral Impact 6-g 100ms**



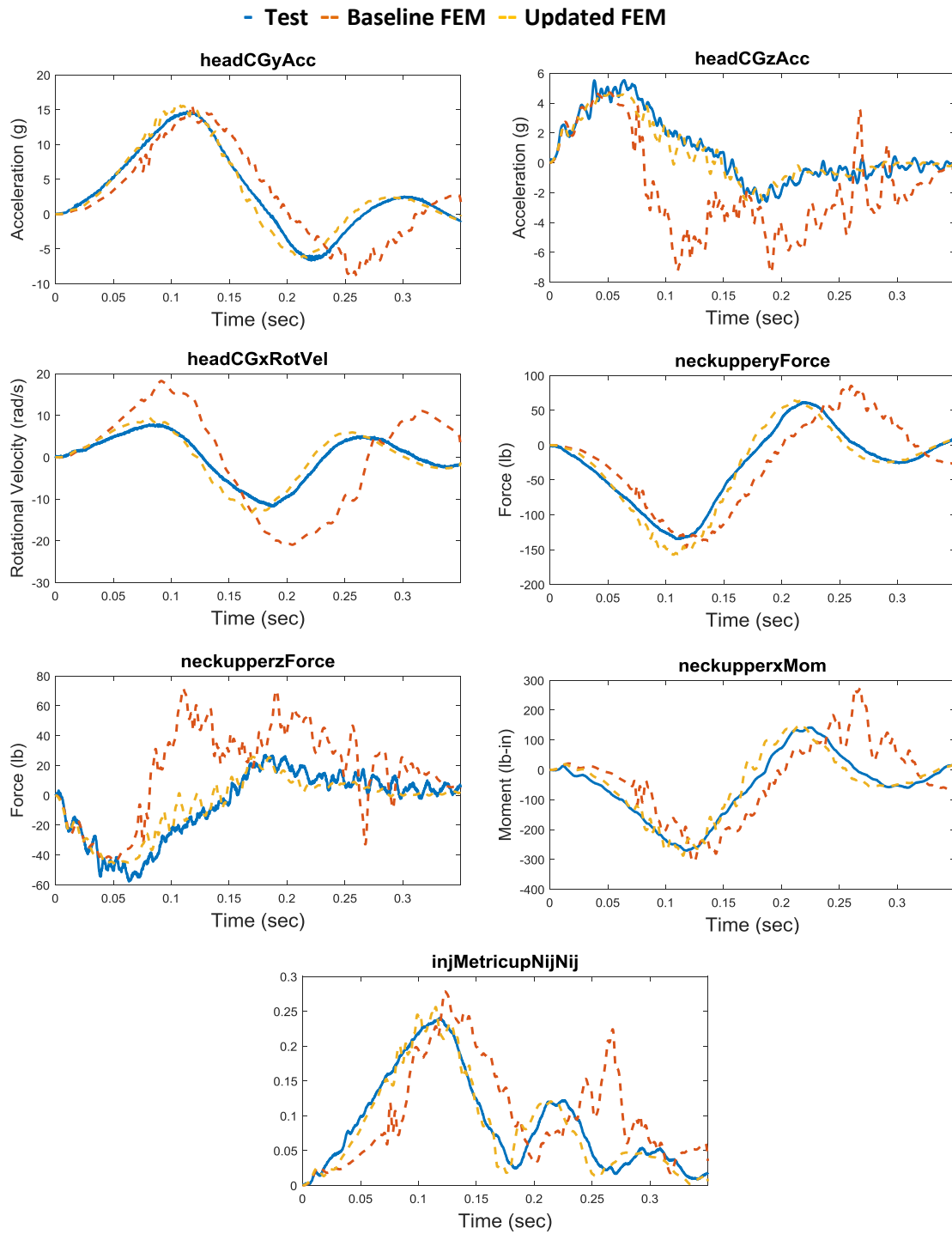
**Figure A15. Test 9737: Lateral Impact 8-g 50ms**



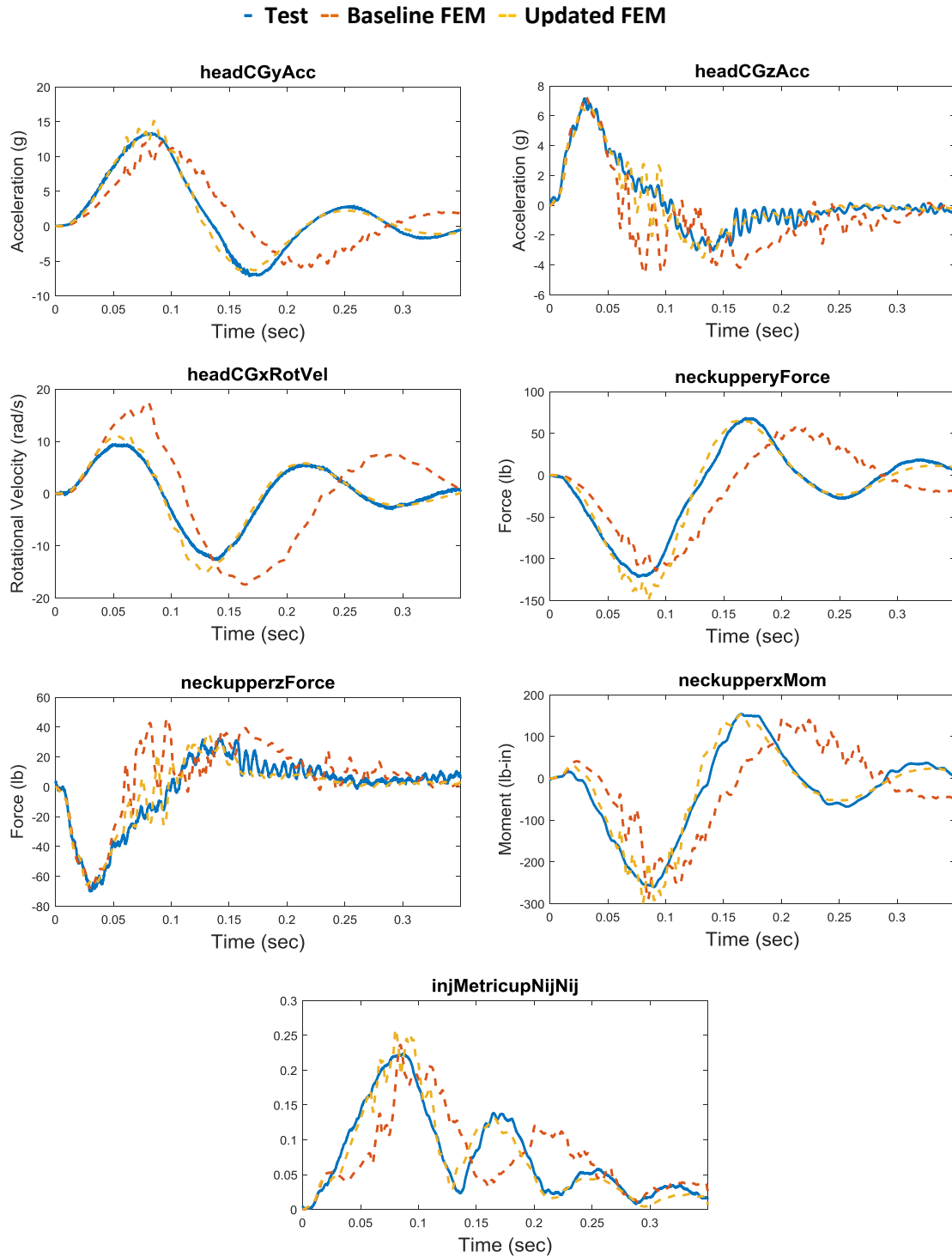
**Figure A16. Test 9739: Lateral Impact 10-g 100ms**



**Figure A17. Test 9739: Lateral Impact 10-g 50ms**

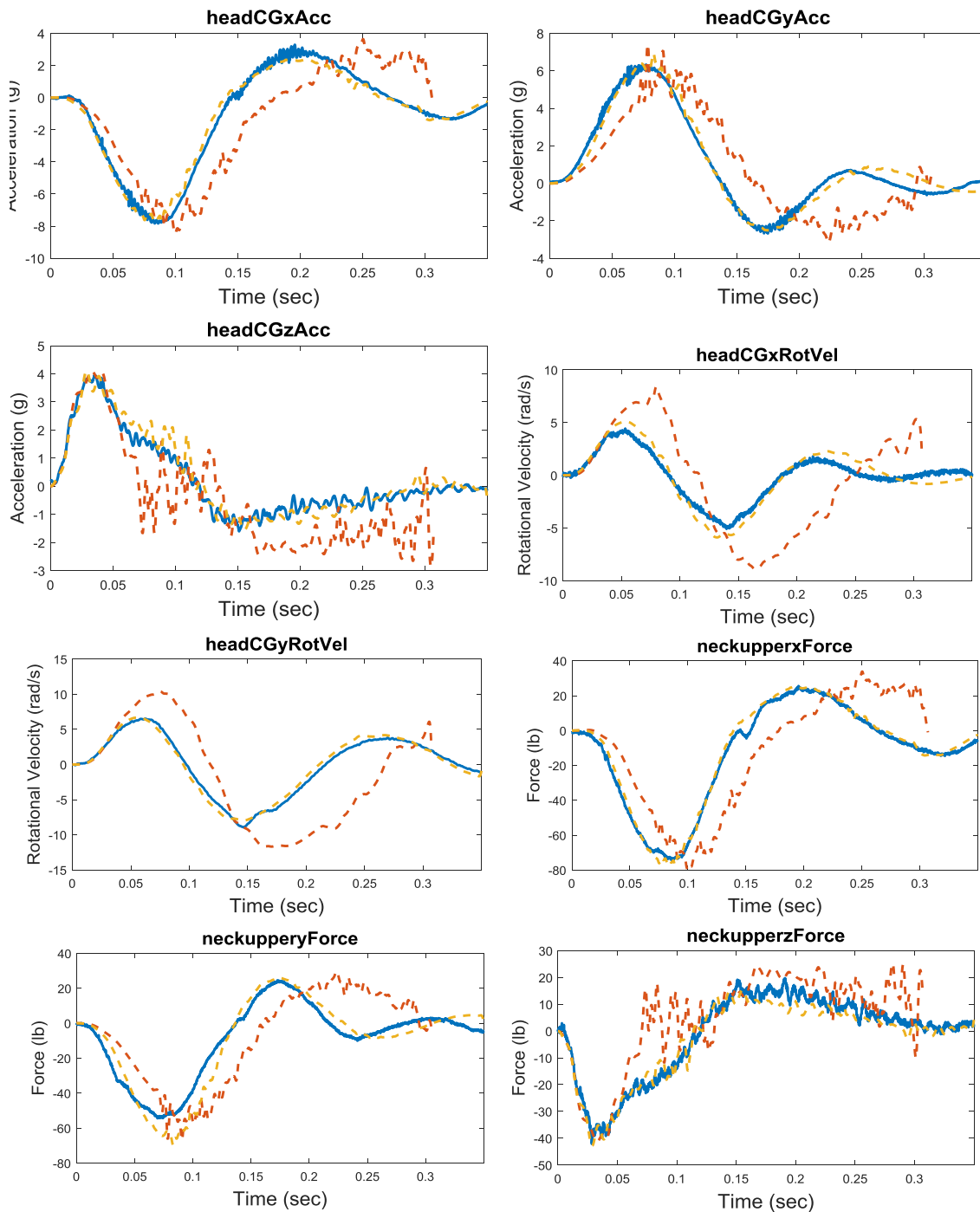


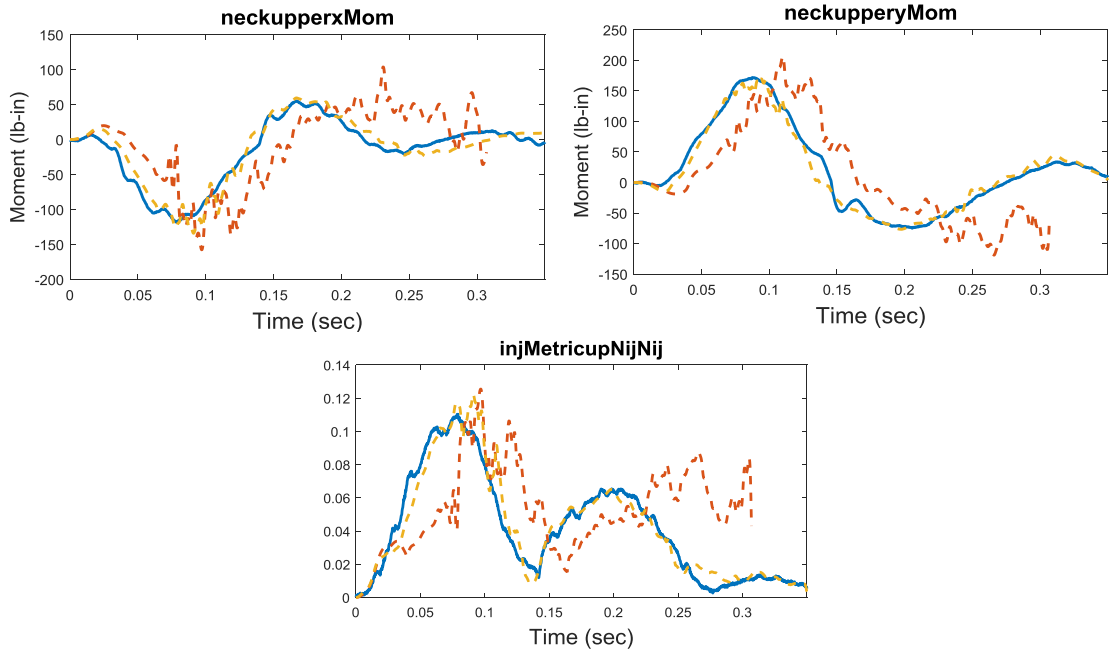
**Figure A18. Test 9714: Lateral Impact 12-g 100ms**



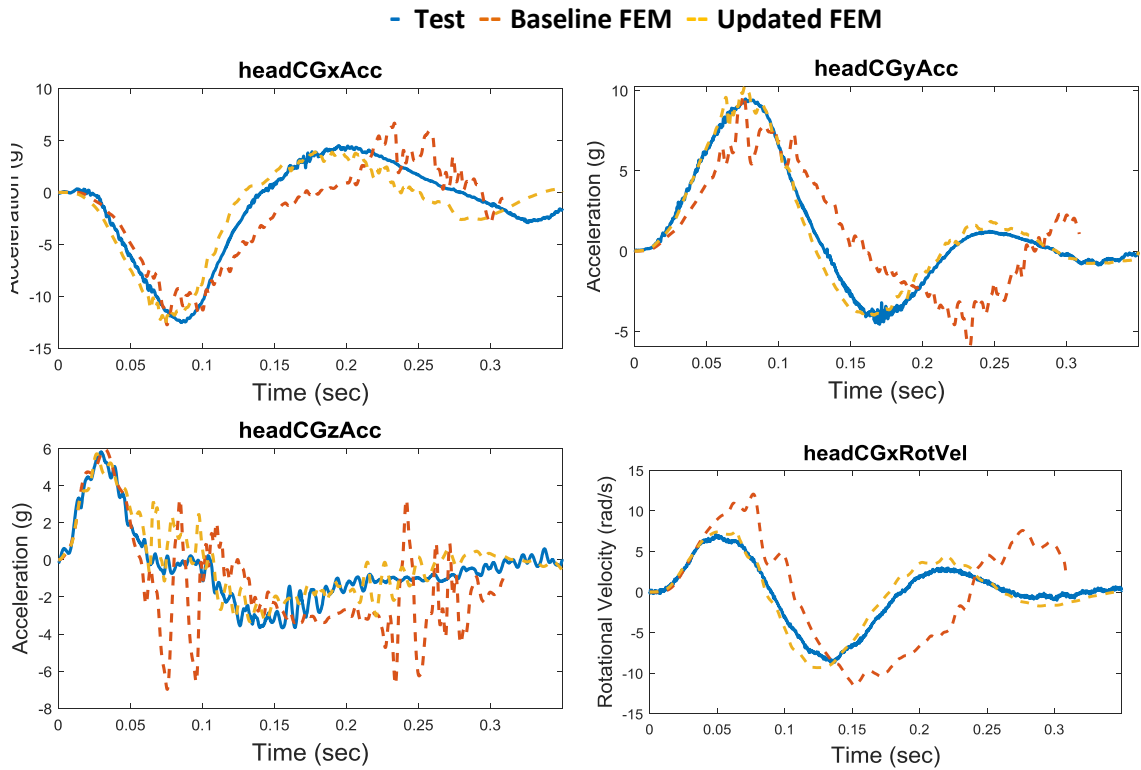
**Figure A19. Test 9738: Lateral 12-g 50ms**

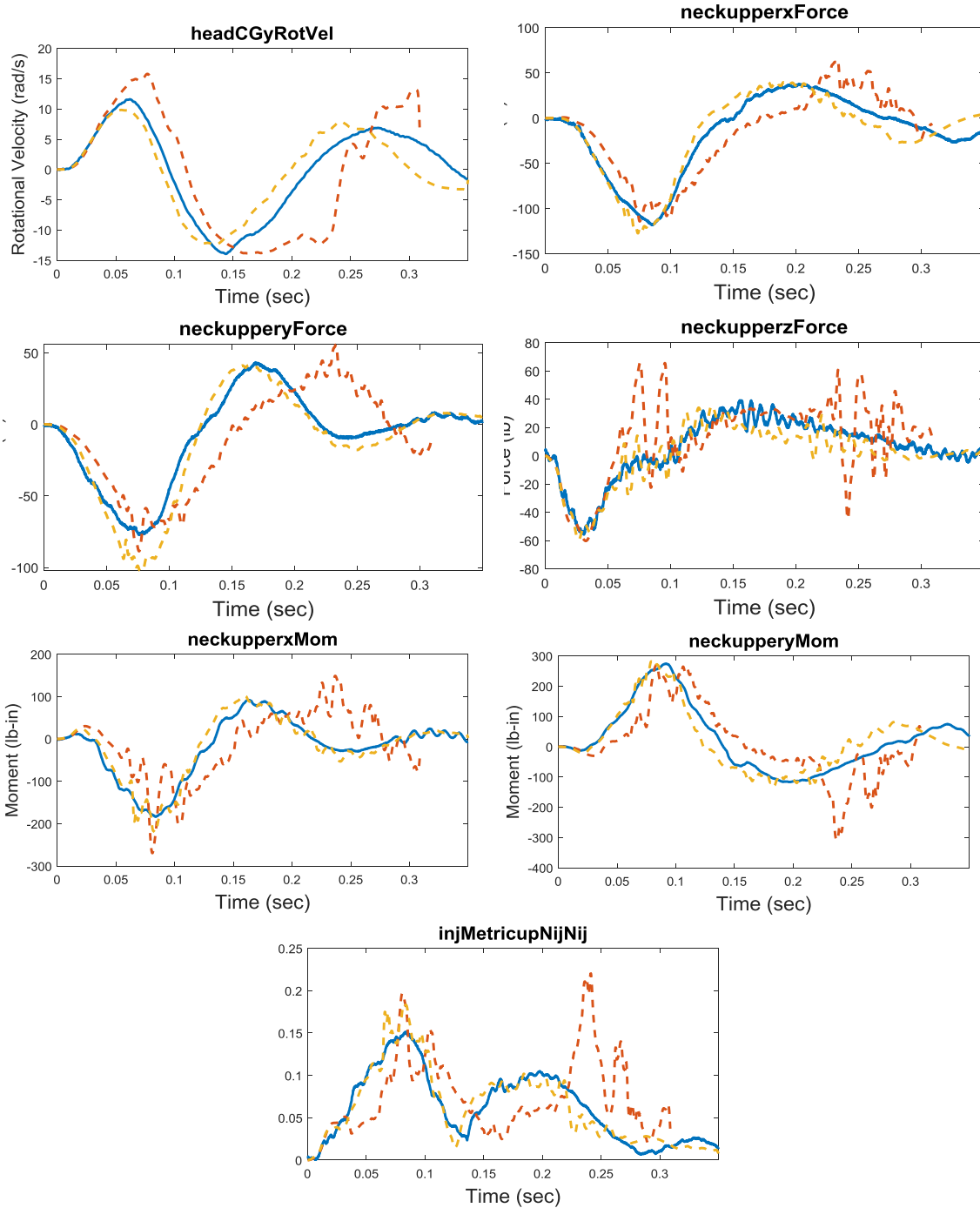
- Test - Baseline FEM - Updated FEM





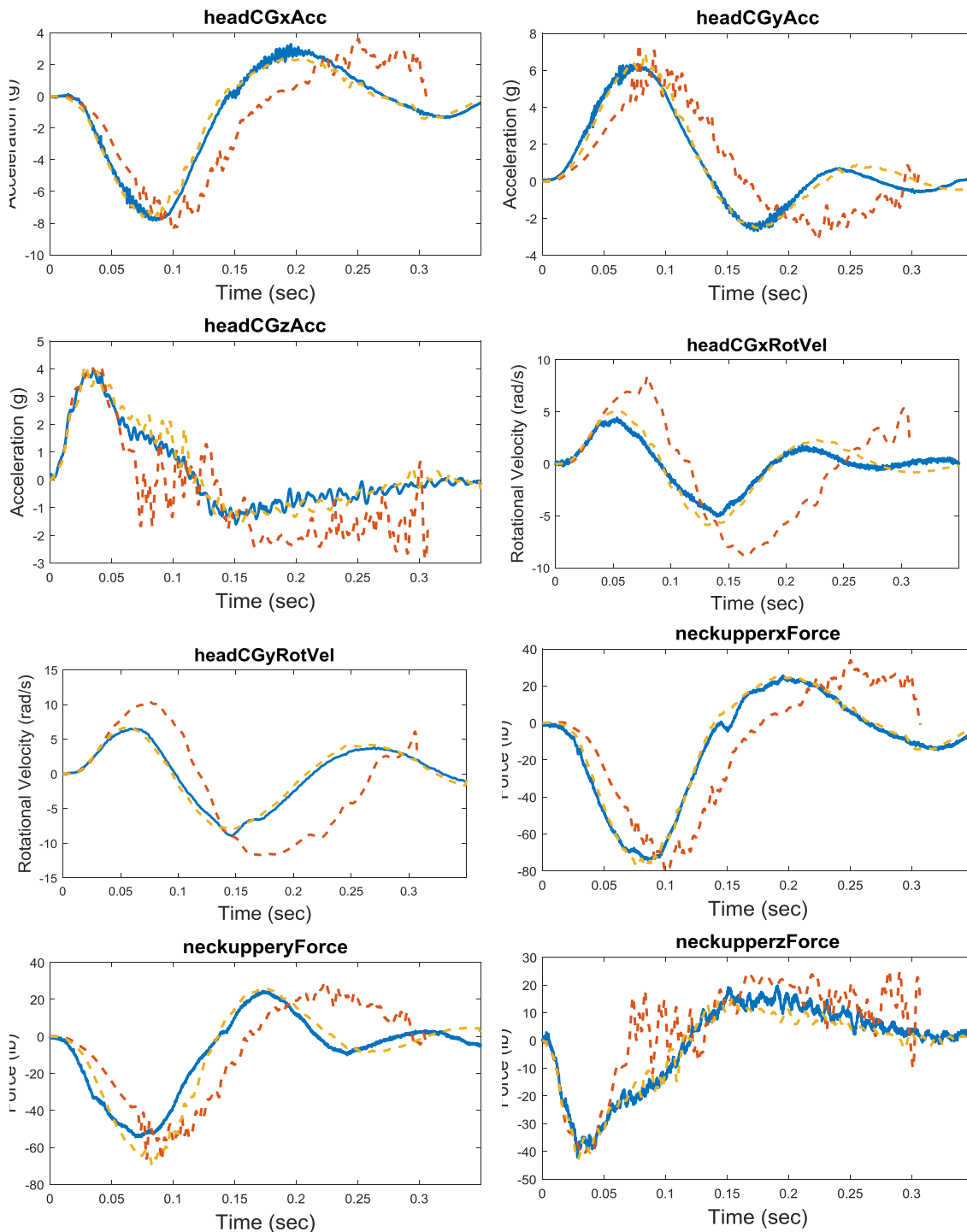
**Figure A20. Test 9743: Combined Frontal-Lateral Impact 8-g 50ms**

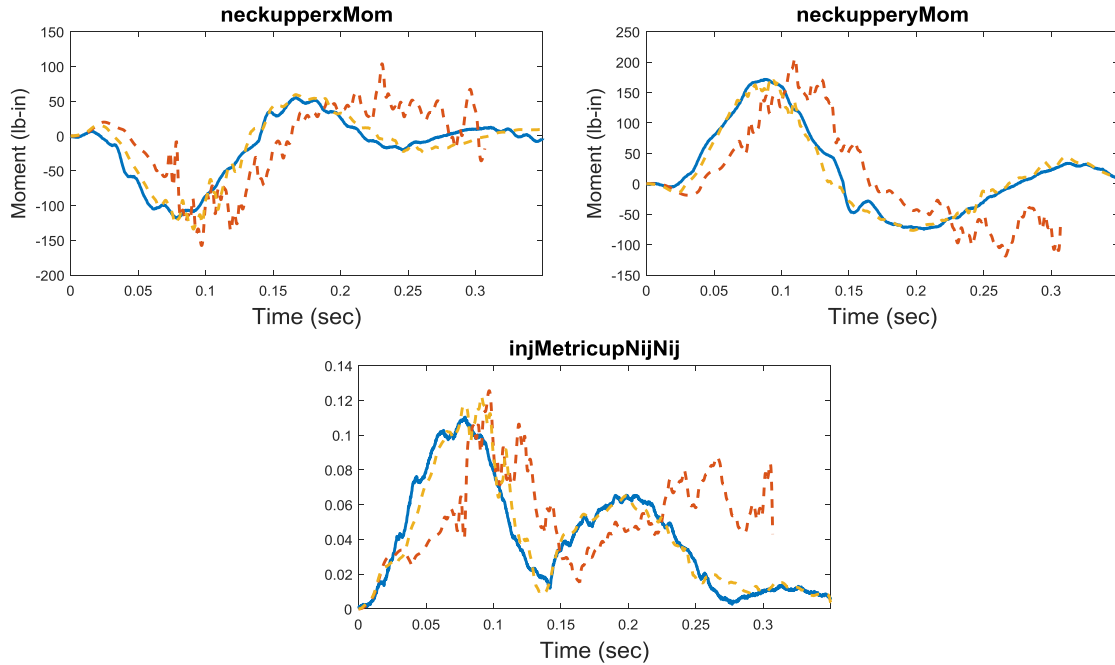




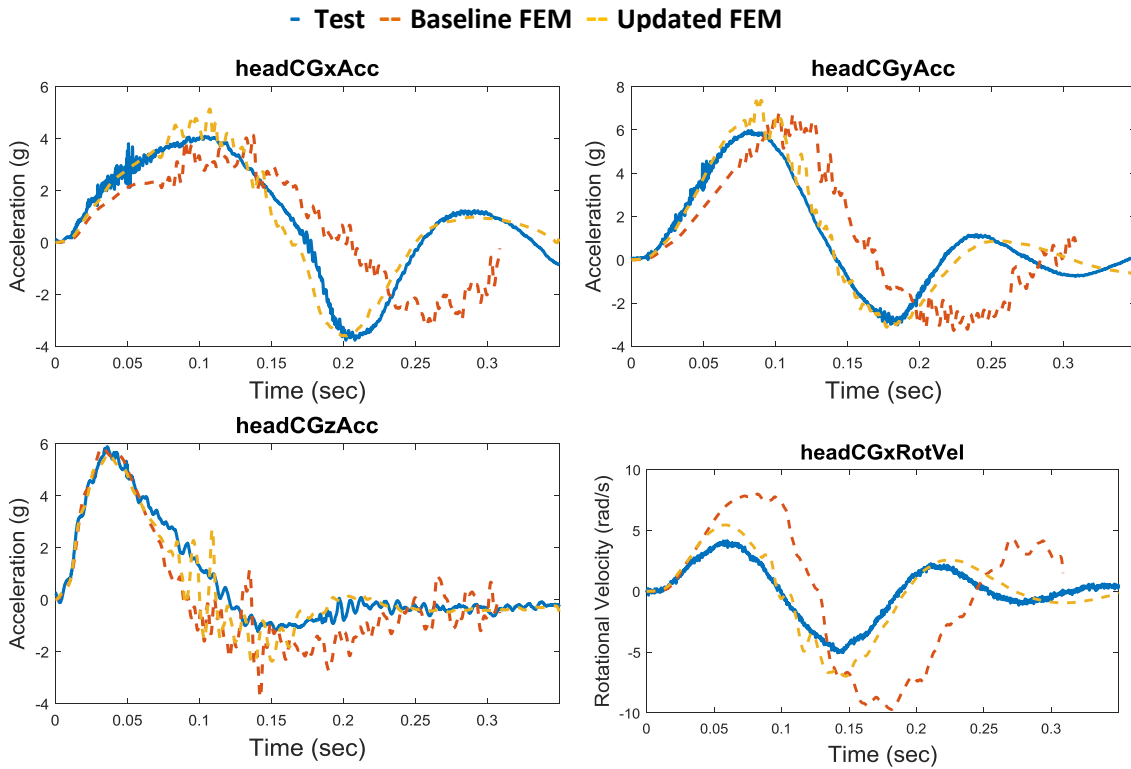
**Figure A21. Test 9744: Combined Frontal Lateral Impact 12-g 50ms**

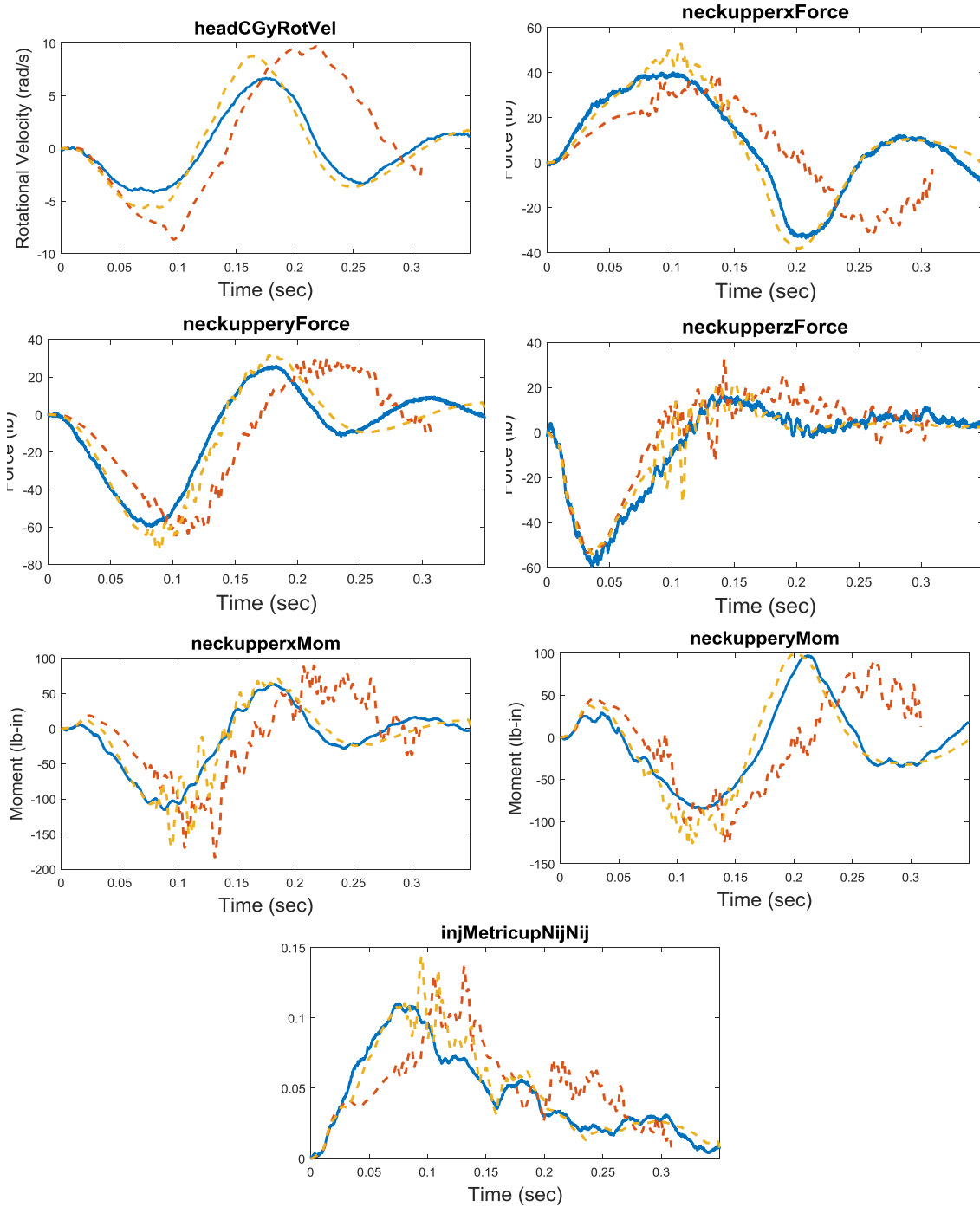
- Test - Baseline FEM - Updated FEM



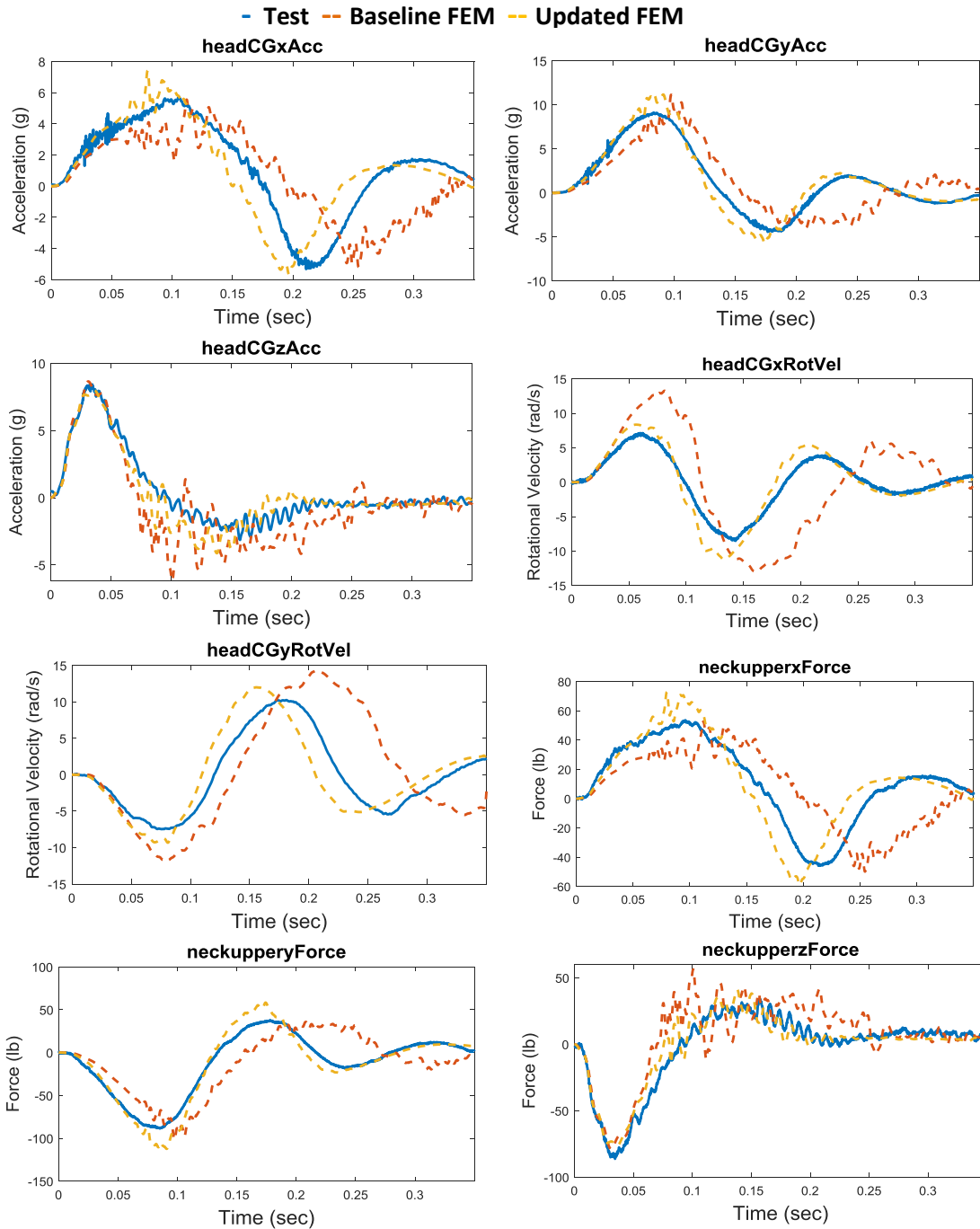


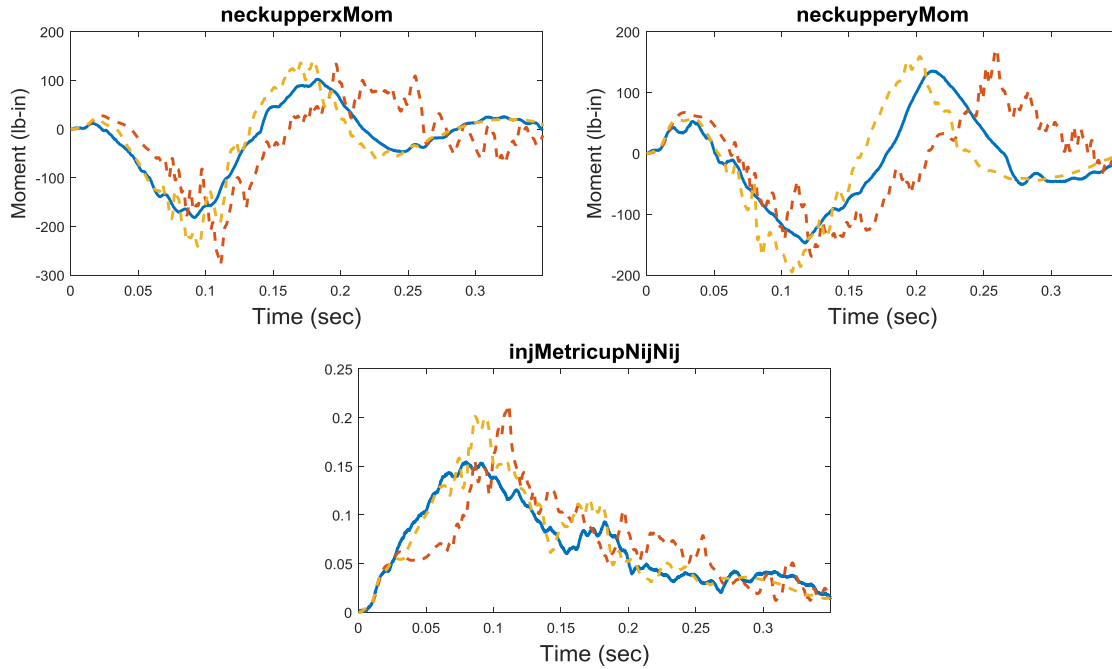
**Figure A22. Test 9745: Combined Frontal-Lateral Impact 16-g 50ms**



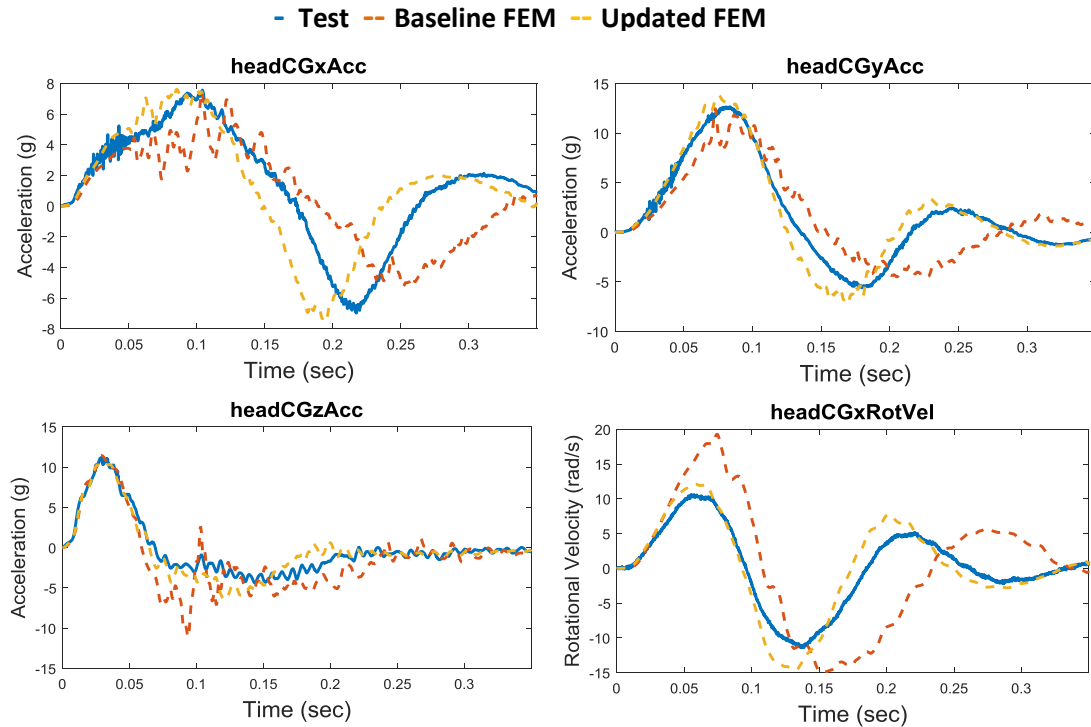


**Figure A23. Test 9746: Combined Rearward-Lateral Impact 8-g 50ms**





**Figure A24. Test 9747: Combined Rearward-Lateral Impact 12-g 50ms**



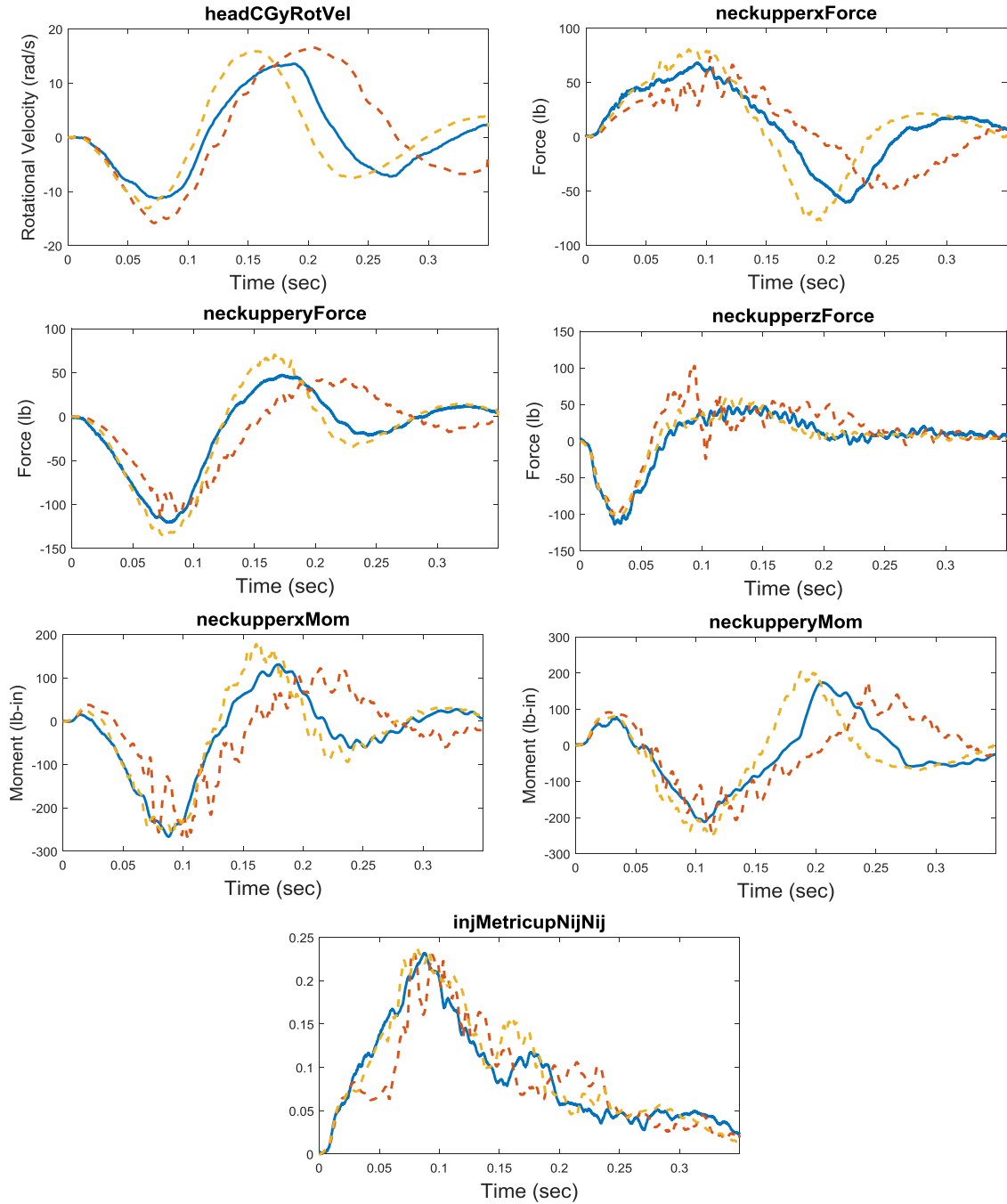


**Figure A25. Test 9748: Combined Rearward-Lateral Impact 16-g 50ms**

**REPORT DOCUMENTATION PAGE**

Form Approved  
OMB No. 0704-0188

The public reporting burden for this collection of information is estimated to average 1 hour per response, including the time for reviewing instructions, searching existing data sources, gathering and maintaining the data needed, and completing and reviewing the collection of information. Send comments regarding this burden estimate or any other aspect of this collection of information, including suggestions for reducing the burden, to Department of Defense, Washington Headquarters Services, Directorate for Information Operations and Reports (0704-0188), 1215 Jefferson Davis Highway, Suite 1204, Arlington, VA 22202-4302. Respondents should be aware that notwithstanding any other provision of law, no person shall be subject to any penalty for failing to comply with a collection of information if it does not display a currently valid OMB control number.  
**PLEASE DO NOT RETURN YOUR FORM TO THE ABOVE ADDRESS.**

<b>1. REPORT DATE (DD-MM-YYYY)</b> 10/04/2019		<b>2. REPORT TYPE</b> Technical Memorandum		<b>3. DATES COVERED (From - To)</b>	
<b>4. TITLE AND SUBTITLE</b> Large Male Anthropomorphic Test Device (ATD) Finite Element Model (FEM) Correlation Improvement				<b>5a. CONTRACT NUMBER</b>	
				<b>5b. GRANT NUMBER</b>	
				<b>5c. PROGRAM ELEMENT NUMBER</b>	
<b>6. AUTHOR(S)</b> Kelly, Michael J.; Somers, Jeffrey T.; Putnam, Jacob B.; Greenhalgh, Preston C.; Lawrence, Charles				<b>5d. PROJECT NUMBER</b>	
				<b>5e. TASK NUMBER</b>	
				<b>5f. WORK UNIT NUMBER</b> 869021.01.07.01.03	
<b>7. PERFORMING ORGANIZATION NAME(S) AND ADDRESS(ES)</b> NASA Langley Research Center Hampton, VA 23681-2199				<b>8. PERFORMING ORGANIZATION REPORT NUMBER</b> L-21064 NESC-RP-19-01416	
<b>9. SPONSORING/MONITORING AGENCY NAME(S) AND ADDRESS(ES)</b> National Aeronautics and Space Administration Washington, DC 20546-0001				<b>10. SPONSOR/MONITOR'S ACRONYM(S)</b>	
				<b>11. SPONSOR/MONITOR'S REPORT NUMBER(S)</b> NASA/TM-2019-220412	
<b>12. DISTRIBUTION/AVAILABILITY STATEMENT</b> Unclassified - Unlimited Subject Category 16 Space Transportation and Safety Availability: NASA STI Program (757) 864-9658					
<b>13. SUPPLEMENTARY NOTES</b>					
<b>14. ABSTRACT</b> As part of an activity for the Commercial Crew Program (CCP), a NASA Engineering and Safety Center (NESC) team conducted tests of small female, medium male, and large male Hybrid III anthropomorphic test device (ATD) head-neck complexes. The results were compared to simulation results from ATD finite element model (FEM) predictions to determine the validity and fidelity of ATD models for use in certifying CCP vehicles. The NESC was requested to help improve the large male ATD FEM to better represent physical responses. This report contains the outcome of the NESC assessment.					
<b>15. SUBJECT TERMS</b> Anthropomorphic Test Device; NASA Engineering and Safety Center; Finite Element Model; Commercial Crew Program					
<b>16. SECURITY CLASSIFICATION OF:</b>			<b>17. LIMITATION OF ABSTRACT</b>	<b>18. NUMBER OF PAGES</b>	<b>19a. NAME OF RESPONSIBLE PERSON</b>
<b>a. REPORT</b>	<b>b. ABSTRACT</b>	<b>c. THIS PAGE</b>			STI Help Desk (email: help@sti.nasa.gov)
U	U	U	UU	60	<b>19b. TELEPHONE NUMBER (Include area code)</b> (443) 757-5802